

110275

ANNUAL REPORT

THE EFFECTS OF CLOUDS ON EARTH RADIATION BUDGET SEASONAL AND INTER-ANNUAL PATTERNS

Pages: 1-4

APPENDIX

1. REPORTS

a. COMMENTS ON THE OCEAN THERMOSTAT

b. DRAFT OF THE PAPER FOR PUBLICATION

**TITLE: CLOUDS, SURFACE TEMPERATURE AND THE TROPICAL
AND SUBTROPICAL RADIATION BUDGET**

c. DRAFT OF PAPER FOR PRESENTATION

**TITLE: SEA-SURFACE TEMPERATURE AND THE SOLAR
IRRADIANCE IN THE TROPICS**

2. ABSTRACT FROM EOS

PRESENTATION OF A PAPER (AGU 1992 SPRING MEETING)

**TITLE: SEA-SURFACE TEMPERATURE AND THE SOLAR
IRRADIANCE IN THE TROPICS**

11-7-92
133176
p 44

ANNUAL REPORT
for
**NATIONAL AERONAUTICS AND SPACE
ADMINISTRATION**

Research Grant No. NAG 5-1012

**Effects of Clouds on the Earth Radiation Budget;
Seasonal And Inter-Annual Patterns**

Principal Investigator:

Dr. Harbans L. Dhuria
Tel. No. (202)-282-3742

NASA Technical Officer:
Code: 916

Dr. H. Lee Kyle
Tel. No. (301)-286-9415

**The University of the District of Columbia
Washington DC 20008
December 24, 1992**

(NASA-CR-191619) EFFECTS OF CLOUDS
ON THE EARTH RADIATION BUDGET;
SEASONAL AND INTER-ANNUAL PATTERNS
Annual Report (District of
Columbia Univ.) 44 p

N93-18870

Unclass

G3/45 0136196

ANNUAL REPORT

THE EFFECTS OF CLOUDS ON EARTH RADIATION BUDGET SEASONAL AND INTER-ANNUAL PATTERNS

The study focussed on Seasonal and regional variations of clouds and their effects on the climatological parameters. The climatological parameters surface temperature, solar insolation, short-wave absorbed, long wave emitted and net radiation were considered. The data of climatological parameters under this study consisted of about 20 parameters of Earth Radiation Budget and Clouds of 2070 target areas which covered the globe. It consisted of daily and monthly averages of each parameters for each target area for the period, June 1979 - May 1980. Cloud forcing and black body temperature at the top of the atmosphere were calculated. Interactions of clouds, cloud forcing, black body temperature and the climatological parameters were investigated and analyzed.

MLCE AND CMATRIX DATABASES

THE Nimbus scanner data, reprocessed by Nimbus Processing Team, was used in our study. The database consisting of thirteen parameters of MLCE and thirty eight parameters of CMATRIX (CLOUD related) of all 2070 target areas of the Globe was developed for our study. However our study mainly focussed on parameters representing the long wave flux, net radiation, albedo, short-wave emitted, insolation, clouds (low, mid and high, cirrus and convective), surface temperature, cloud top temperature, cloud forcing and solar irradiance.

ACCOMPLISHMENTS:

As a result of this study the following tasks have been completed or are in progress:

(a) PRESENTATION OF A PAPER

A paper on "SEA-SURFACE TEMPERATURE AND THE SOLAR IRRADIANCE IN THE TROPICS" was presented at American Geophysical Union (AGU) Spring (May 14 - 17) 1992 meeting in Montreal. A draft of the report on the relationship between the Sea-Surface Temperature and the Solar Irradiance in the Tropics was prepared for presentation at AGU meeting. The report of the paper for presentation and the abstract of the paper which was published in EOS are enclosed.

(b) PREPARATION OF ATLAS

Annual Contour plots (more than 120) of selected parameters and for latitudes bands of tropics and subtropics and higher latitudes for the Atlas were constructed. However only plots for selected latitudinal bands will be included in the Atlas.

(c) CORRELATIONAL STUDY

Correlational study of selected climatological parameters and clouds was performed by constructing the Global character and contour plots.

(d) REPORT BASED ON THE RECENT JOURNAL ARTICLES

Based on the literature, related recent articles that appeared in the journals and based on our study a report "COMMENTS ON THE OCEAN THERMOSTAT" was prepared and it is included with this report.

(e) DRAFT OF THE PAPER FOR PUBLICATION

A preliminary draft of the paper entitled "CLOUDS, SURFACE TEMPERATURE, AND THE TROPICAL AND SUBTROPICAL RADIATION BUDGET" for future publication was prepared. The paper for publication will also include the analysis of the two more years of ERBE and ISCCP data for the period February 1985 to January 1987 for appropriate results and validation. This paper for publication thus depends on the next phase of the study.

Last year the Summer and Fall annual variation maps of these parameters were made and they were analyzed for 16 latitude zones, each 4.5° of latitude in width, from 36° North to 36° South latitude. Particular attention was paid to the Ocean. Over the oceans the fairly uniform regional surface albedo and temperature makes it easier to study the interaction between the clouds and the regional radiation budget. There are strong interactions but these vary depending upon cloud types and amounts. In turn both cloud types and amounts are related to the surface temperature and the general atmospheric circulation pattern.

DEVELOPMENT OF SOFTWARE

Until July 1992, Computer programs were developed on the NASA/GODDARD IBM 9021 mainframe. NCAR graphic package was used for obtaining the contour plots for the ATLAS and other global plots for analysis. Several plots were also generated for analyzing and interpreting the interactions of the parameters under study.

But in August 1992 the NCAR Graphic Software package support was withdrawn from IBM computer and this graphic package was made available on SUPER COMPUTER CRAY Y-MP. Some extra time had to be used for understanding new technology and in understanding the use of new computer system, transferring the software from IBM computer to CRAY and rewriting some of the software for the study.

The Principal Investigator continued his study and overcame the problem that arose due to changes in the use of the computer systems and software by requesting the AT-NO-COST EXTENSION of the research grant period.

STATUS OF THE STUDY

The study continued according to the guidelines in the proposal, however the research also focussed on the meetings and discussions with the NASA technical monitor Dr. H. L. Kyle and colleagues who are involved in the related research work.

DATABASE FOR THE CONTINUING STUDY

Database consisting of Earth Radiation Budget Experiment (ERBE) from S-4 tapes and International Satellite Cloud Climatology Project (ISCCP) from C2 tapes covering the two-year period from February 1985 to January 1987 has been organized on four cassette tapes. The database which represents the Global, 2.5° latitude/longitude spatial resolution of monthly parameters' fields was extracted from ERBE and ISCCP input tapes. The data was merged by target area (target area = 2.5° Latitude x 2.5° Longitude) for each month.

ERBS/NOAA-9/NOAA-10 ERBE data products were the source of ERBE data for all months except the last three for which the three-satellite ERBS/NOAA-9/NOAA-10 ERBE

product was used. Because of the large data volume, the final product (database) is stored on four 3480 square tape cartridges that currently reside on the NASA/GODDARD IBM 9021 mainframe computer. Each cartridge contains six 32 megabyte files, one for each of six months, for a total of 192 megabytes representing the data of two years.

Both the higher resolution 2.5° data and 5.0° data of 24 months were stored on the four tapes. The ERBE and ISCCP data were ordered through the National Space Science Data Center (NSSDC) by Dr. Lee Kyle. These data, after re-mapping to the 2.5° equal-angle ERBE grid (10368 target areas) were merged with ERBE data by months to form the final product.

FUTURE PLANS COVER:

- * Study and analyze multi-variables correlations of the ERB AND CLOUD products.
- * Examine additional data sets such as the Earth Radiation Budget Experiment and Clouds for the period February 1985 - January 1987 for analysis and interpretation of results.
- * Presentation of a Paper at AGU Spring 1993 meeting.
- * Preparation of a paper for publication based on the results obtained from the present study and the study based on the analysis and interpretation of the data of 10368 target for the period from February 1985 to January 1987.

ANNUAL REPORT

THE EFFECTS OF CLOUDS ON EARTH RADIATION BUDGET SEASONAL AND INTER-ANNUAL PATTERNS

Pages: 1-4

APPENDIX

1. REPORTS

- a. COMMENTS ON THE OCEAN THERMOSTAT
- b. DRAFT OF THE PAPER FOR PUBLICATION

TITLE: CLOUDS, SURFACE TEMPERATURE AND THE TROPICAL
AND SUBTROPICAL RADIATION BUDGET

- c. DRAFT OF PAPER FOR PRESENTATION

TITLE: SEA-SURFACE TEMPERATURE AND THE SOLAR
IRRADIANCE IN THE TROPICS

- ##### **2. ABSTRACT FROM EOS PRESENTATION OF A PAPER (AGU 1992 SPRING MEETING)**

TITLE: SEA-SURFACE TEMPERATURE AND THE SOLAR
IRRADIANCE IN THE TROPICS

COMMENTS ON THE OCEAN THERMOSTAT

Harbans L. Dhuria
University of the District of Columbia, Washington, DC

H. Lee Kyle
NASA/Goddard Space Flight Center, Greenbelt, MD

December 1992

Our investigation of the seasonal variation of the tropical radiation budget has brought forth new evidence concerning the relationship between clouds and the sea-surface temperature (SST). As is well known, the monthly mean SST rarely exceeds 303 K. Ramanathan and Collins (1991) have proposed a cirrus cloud/radiation budget feedback mechanism which, they estimate, should keep the SST from exceeding 305 K. Stephens and Slingo (1992) point out that on the large scale the tropical SST seems to be chiefly maintained by coupled ocean and atmosphere circulation patterns. However, they say that while more information is needed to decipher the exact mechanisms, the Ramanathan's and Collins' hypothesis is intriguing. Our study indicates that large-scale phenomena are dominant, but that the cloud feedback mechanism appears to be important.

The Ramanathan and Collins mechanism relies on atmospheric deep convective activity over warm water pools to spin off a thick cirrus cover which, in turn, sharply reduces the solar radiation absorbed at the surface. This keeps the SST from rising further. The evidence indicates that in these tropical warm water pools, the mean regional top-of-the-atmosphere net radiation (NR) decreases only a small amount when the deep convective clouds form (see for instance Dhuria and Kyle (1991)).

$$NR = ASW - OLR$$

where

ASW = absorbed shortwave solar radiation

OLR = (Earth-emitted) outgoing longwave radiation, all quantities at the top-of-the-atmosphere

The high clouds sharply reduce both ASW and OLR, but the net radiation changes little. However, in the clear sky case, most of the heating occurs at the surface, while in deep convective cloud fields a great deal of heating occurs in the mid- and upper troposphere. In the Ramanathan and Collins theory, atmospheric circulation removes enough heat from the cloud layers to aid in the cooling process.

Our evidence indicates that while radiative processes are regionally important, other factors must be considered. We compared the Nimbus-7 Earth radiation budget (ERB) and cloud products for the period June 1979 through May 1980 (Kyle et al., 1990; Stowe et al., 1988). The cloud products include quality controlled Air Force 3D nephanalysis surface temperatures. Time- and space-averaged ERB and cloud products are formed on an approximately equal area world grid, each region about $(500 \text{ km})^2$ in size. Along the Equator, the regions are 4.5° latitude, longitude

squares. Figures 1 and 2 compare two Pacific Ocean regions just south of the Equator. The first region centered at (2.25°S latitude, 159.75°E longitude) lies in the western pacific warm water pool. This is an equatorial rain region and normally has a 70% to 90% cloud cover with high and medium altitude clouds dominant. The second region centered at (2.25°S, 92.25°W) is a cool water region just off the coast of South America where low stratus clouds predominate. Our equatorial study actually includes nine regions in the Western Pacific rain region and ten in the Eastern Pacific cool water region. The two regions shown in the figures are each characteristic of their neighboring region.

The figures compare monthly averages throughout the year. Figure 1 shows the top-of-the-atmosphere insolation, net radiation, total noon cloud cover, the diurnally averaged albedo, and the noon surface temperatures. Note that the surface temperature in the Western Pacific is always 4° to 6° warmer than in the East even in February through April when the Eastern Pacific absorbs much more solar energy than does the cloud shrouded Western Pacific. In the Eastern Pacific, the surface temperature is dominated by the wind-assisted upwelling of deep cold water plus the cold Humbolt surface current. The modest 14% seasonal variation in the insolation is associated with important changes in cloud amount and type in the two regions. These changes, in turn, influence the cloud forcing (Figure 2). The cloud forcing used here is defined as the difference (mean-clear sky) observed top-of-the-atmosphere longwave, shortwave, and net radiation fluxes (Ramanathan, 1987). By this definition, the longwave cloud forcing is positive and the reflected shortwave forcing is negative. The net radiation forcing is the sum of the other two forcing terms.

In the Western Pacific, both the clouds and the shortwave forcing move roughly in phase with the insolation. Thus, even though the net radiation is 30 or 40 W/m² higher in March than in June, the solar energy absorbed at surface has somewhat decreased. The excess energy is absorbed in the atmosphere. Unfortunately, we cannot definitely state how the surface net radiation varies. As the clouds thicken, the downward longwave flux should increase. The analysis of Darnell et al., (1992) for the months of July and October 1983 and January and April 1984 does indicate that the net surface flux should increase from July to January in both the Eastern and Western Pacific regions we studied. However, as with the top-of-the-atmosphere values (see Figure 1), the increase should be much larger in the Eastern region. In the Western Pacific, the surface temperature is nearly consistent throughout the year with a value just below 30°C (303 K). However, as the clouds thicken, there is a tendency for the surface temperature to slightly decrease although the cloud and temperature changes are not perfectly in phase. This is roughly what we should expect from the hypothesis of Ramanathan and Collins. However, bordering the warm water rain center, in both the Pacific and Indian oceans, are regions with thinner clouds and, hence, higher absorbed solar radiation and net radiation than in the rain center. Here the surface temperature behaves seasonally in a manner similar to that in the rain center except that it averages about 0.3°C lower. Thus, though cloud feedback is not negligible, other processes are obviously at work.

In the Eastern Pacific, cool water region, it is tempting to connect the February and March solar insolation maximum with the cloud minimum and temperature maximum. However, a complete picture should also include the ocean currents and the atmospheric winds and water vapor.

In conclusion, it appears that cloud feedback mechanisms are important, but not dominant factors. The surface temperature differential between the Eastern and Western Pacific is a strong example of nonradiation balance force at work. In the Western Pacific itself, the highest temperatures tend to be associated with the thickest cloud cover but not the highest net radiation or absorbed solar radiation. Again strong, nonradiation balance, forces appear at work. Qualitatively, there is undoubtedly a sort of a thermostat effect. When a monsoon system develops, it uses up a great deal of energy, but the cirrus shield which blocks incoming solar energy appears to be just part of the picture.

References:

- Darnell, W. L., W. F. Staylor, S. K. Gupta, N. A. Ritchey, and A. C. Wilber, 1992: Seasonal Variation of Surface Radiation Budget Derived From the International Satellite Cloud Climatology C1 data, *J. Geophys. Res.*, **97**, 15,741-15,760.
- Dhuria, H. L. and H. L. Kyle, 1990: Cloud Types and the Tropical Earth Radiation Budget, *J. Climate*, **3**, 1409-1434.
- Kyle, H. L., R. R. Hucek, B. Groveman, and R. Frey, 1990: User's Guide: Nimbus-7 Earth Radiation Budget Narrow-Field-of-View Products, NASA RP-1246, 76 pages.
- Ramanathan, V., 1987: The Role of Earth Radiation Budget Studies in Climate and General Circulation Research, *J. Geophys. Res.*, **92**(4), 4075-4095.
- Ramanathan, V. and W. Collins, 1991: Thermodynamic Regulation of Ocean Warming by Cirrus Clouds Deduced From Observations of the 1987 El Niño, *Nature*, **351**, 27-32.
- Stephens, G. and T. Slingo, 1992: An Air Conditioned Greenhouse, *Nature*, **358**, 369-370.
- Stowe, L. L., C. G. Wellemeyer, T. F. Eck, H. Y. M. Yeh, and the Nimbus-7 Cloud Data Processing Team, 1988: Nimbus-7 Global Cloud Climatology, Part I: Algorithms and Validation, *J. Climate*, **1**, 445-470.

Figure Captions:

Figure 1. Seasonal variations in the insolation, total noontime cloud cover, diurnally averaged albedo and net radiation, and the noontime surface temperature are compared for two equatorial Pacific Ocean regions. One centered at 159.75°E longitude in the western Pacific is in an equatorial rain region. The other centered at 92.25°W longitude in the eastern Pacific lies off the coast of South America. Monthly averages are plotted.

Figure 2. As in Figure 1, but here longwave, shortwave and net cloud forcing terms are plotted.

Figure 1 and 2 Comparison of warm and cool equatorial ocean regions.

OCEAN (2.25°S LATITUDE)

LONGITUDES (159.75°E and 92.25°W)

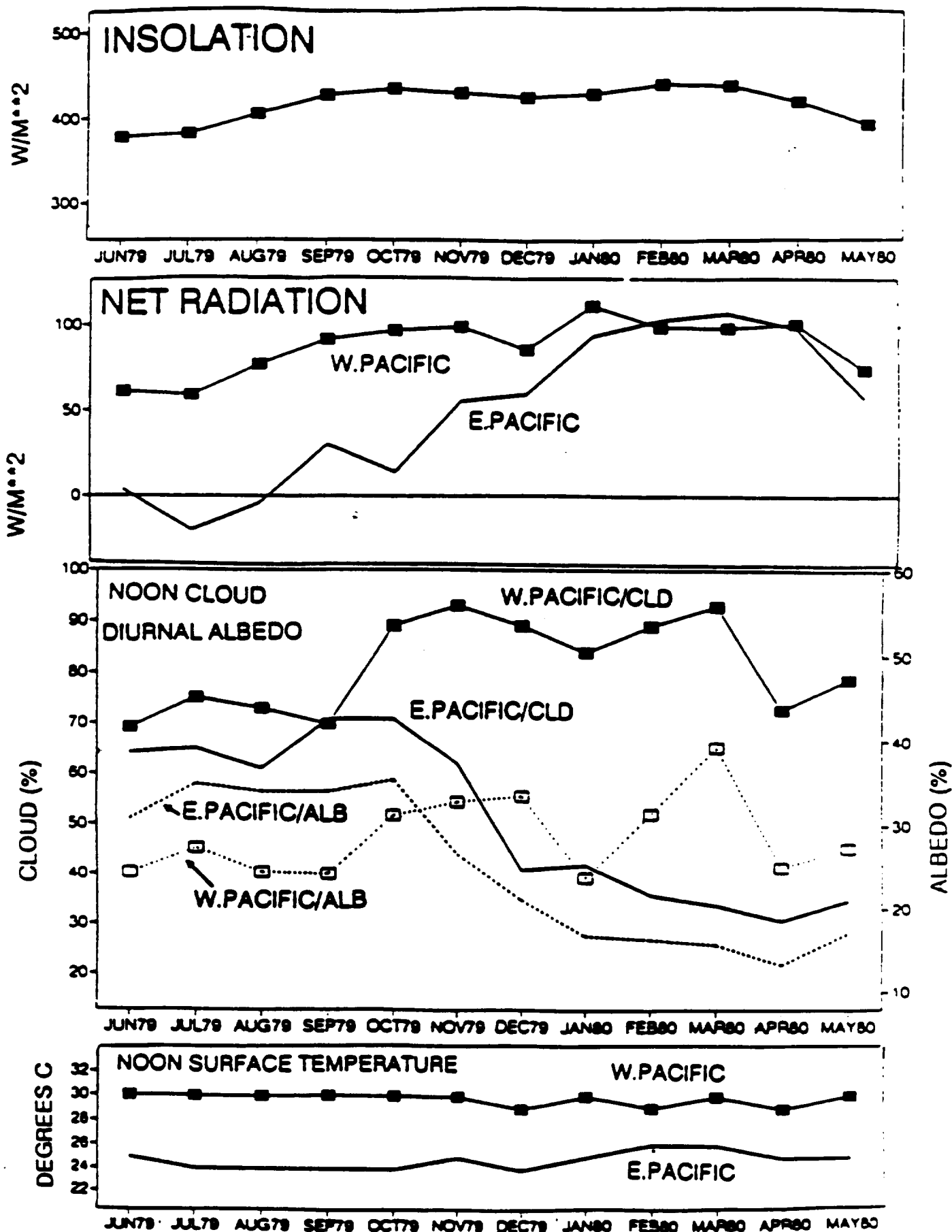


Figure 1

OCEAN (2.25°S LATITUDE)

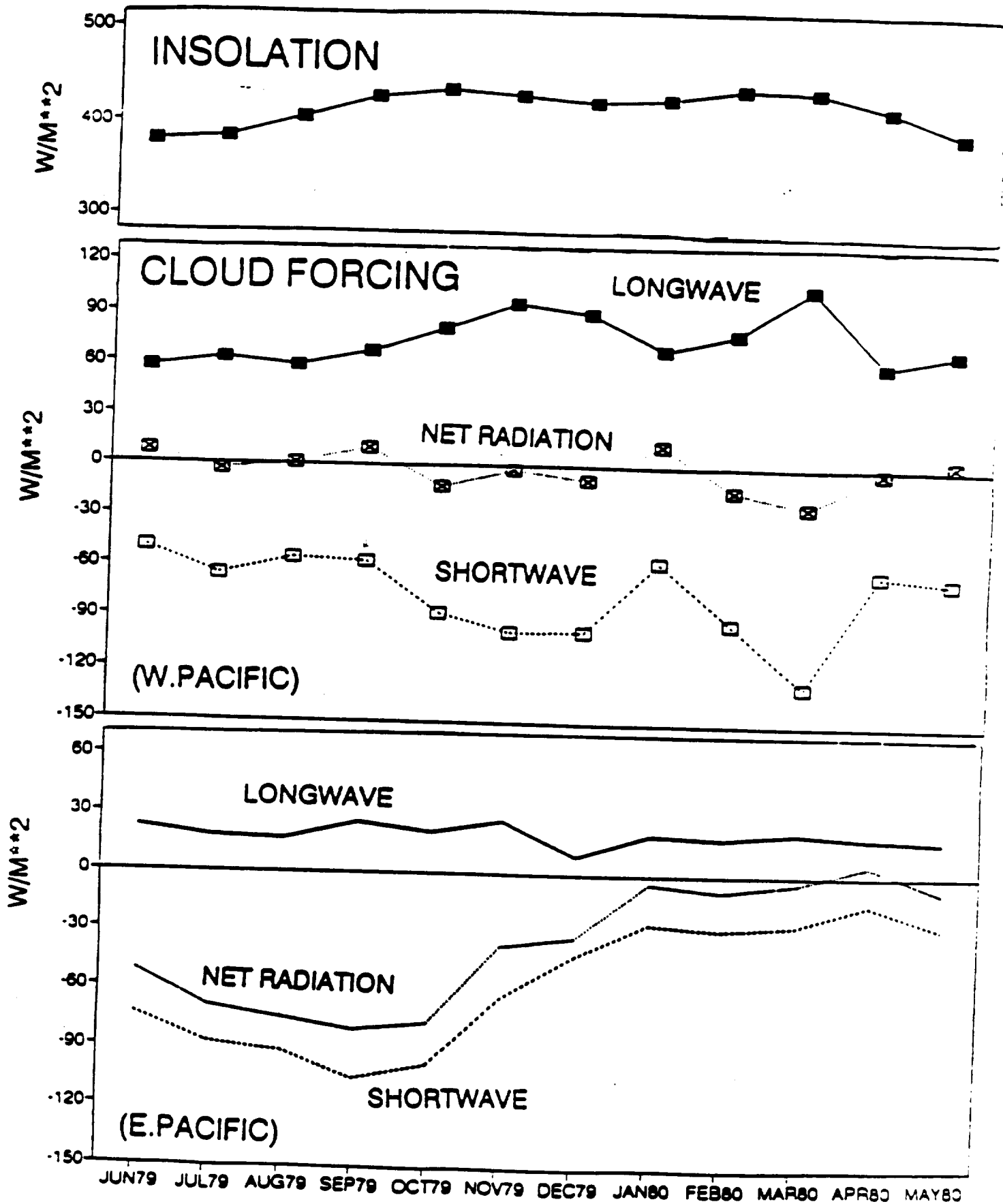


Figure 2

CLOUDS, SURFACE TEMPERATURE, AND THE TROPICAL AND SUBTROPICAL RADIATION BUDGET

Harbans L. Dhuria
University of the District of Columbia, Washington, DC

H. Lee Kyle
NASA/Goddard Space Flight Center, Greenbelt, MD

1. INTRODUCTION

The solar energy drives both the Earth's climate and biosphere, but the absorbed energy is unevenly distributed over the Earth. The tropical regions receive excess energy which is then transported by atmospheric and ocean currents to the higher latitudes. All regions at a given latitude receive the same top of the atmosphere solar irradiance (insolation). However, the net radiation received from the Sun in the tropics and subtropics varies greatly from one region to another depending on local conditions. Over land, variations in surface albedo are important. Over both land and ocean, surface temperature, cloud amount, and cloud type are also important. This study uses the Nimbus-7 cloud and Earth radiation budget (ERB) data sets to examine the affect of these parameters on the radiation over the course of 1 year (June 1979 to May 1980).

Clouds are the most important and also the most variable moderator of the radiation budget. The four components of the planetary radiation budget are the top-of-the-atmosphere (TOA): insolation (solar irradiance), outgoing longwave radiation (OLR), absorbed shortwave (ASW), and net radiation (NR). They are connected by the equation:

$$NR = (I - A)I_s - OLR \quad (1)$$

where:

I_s is the insolation

A is the albedo, and

$ASW = (I-A)I_s$ is the absorbed shortwave radiation

Several studies, using satellite data, have recently examine the effects of clouds on the radiation budget (see for instance Arking, 1991; Ardanuy et al., 1991; Harrison et al., 1990; Hartmann and Doelling, 1991; and Dhuria and Kyle, 1990). Low thick clouds sharply reduce the absorbed, but only slightly reduce the emitted radiation; thus, they strongly decrease the net radiation. Conversely, thin, high-altitude cirrus clouds can increase the net radiation by only slightly reducing the absorbed while strongly reducing the emitted radiation. In the global mean, clouds reduce the net radiation received from the Sun. However, in the tropics, clouds can regionally either increase or decrease the net radiation depending on cloud type and amount. In the mean, clouds just slightly decrease the tropical net radiation.

Of course, cloud types and amount are dependent on the regional climate and, in particular, on the surface temperature. Thus, some relationship between the regional surface temperature and net radiation might be suspected. In fact, the cooler regions generally have a lower net radiation than do the warmer ones. They also tend to show a different pattern for the seasonal cycle of the radiation budget parameters. These differences in the tropics and subtropics are examined in this study over the course of 1 year (June 1979 to May 1980). The Nimbus-7 cloud and Earth radiation budget scanner data are briefly described in Section 2, Section 3 gives an overview of the problem based on annual means, while seasonal variations are discussed in Section 4. A summary and discussion come in Section 5.

2. THE NIMBUS-7 CLOUD AND EARTH RADIATION BUDGET DATASETS

The Nimbus-7 satellite was launched into a stable, nearly circle, Sun-synchronous orbit on October 24, 1978. The mean spacecraft altitude is 955 km, the orbit period is 104 minutes, and equator crossings are a little before noon and midnight local time. The spacecraft carried into orbit a diverse complement of scientific instruments, three of which contributed to this study: the Earth Radiation Budget (ERB), the Temperature and Humidity Infrared Radiometer (THIR), and the Total Ozone Mapping Spectrometer (TOMS).

The ERB experiment (Jacobowitz et al., 1984), itself, contains three different sensor groups: a solar telescope, a set of wide-field-of-view (WFOV) Earth flux sensors, and a narrow-field-of-view (NFOV) scanner. Separate Earth radiation budget datasets were derived from the WFOV and NFOV measurements. The scanner has the better spatial resolution with a nadir footprint about 90 km x 90 km). The scanner failed on June 22, 1980, but the WFOV and solar sensors are still taking measurements. The total solar irradiance measurements are still being released (Hoyt et al., 1991), but due to budget constraints, the final calibration of the WFOV measurements stopped after data month October 1987.

Some algorithm problems degraded the quality of the original scanner Earth radiation budget products (Kyle et al., 1985). Improved algorithms were recently used to reprocess 13 months (May 1979 to May 1980) of the scanner measurements (Ardanuy et al., 1990). It is this reprocessed product that is used in this study. The Earth radiation budget parameters considered include daily and monthly averaged TOA insolation and both clear and average sky albedo, emitted and net radiation.

The Nimbus-7 cloud dataset (Stowe et al., 1988,1989) is derived from the THIR 11.5- μm infrared (IR) and the TOMS 0.36- and 0.38- μm ultraviolet (UV) measurements. The THIR nadir footprint has a resolution of 6.7 km, while TOMS channels have a (50 km x 50 km) nadir footprint. The TOMS channels used are not affected by ozone absorption. Separate IR and UV estimates of cloud amount are made. The IR uses the 11.5- μm measurements, concurrent Air Force nephelometer surface temperatures and regional climatological atmospheric temperature lapse rates. This allows both day and night IR cloud estimates to be made. UV cloud estimates are made only during daylight when the Air Force nephelometer reports no snow or ice in the region. For daylight periods, the separate estimates are combined by an algorithm that gives most weight to the IR estimate for mid- and high-level clouds. However, for low clouds the UV estimate is given considerable weight. From this dataset, we used the bispectral cloud estimates, the Air Force surface temperatures, and the average clear scene and cloud top IR radiances.

ERB and cloud datasets we used consisted of daily and monthly averages on an approximately equal area global grid. It consisted of 2070 regions each about (500 km x 500 km) in size. Near the equator, regions are 4.5° latitude by 4.5° longitude. Annual means are obtained by averaging the monthly means.

3. MEAN ANNUAL RELATIONSHIPS

In the annual mean, the central half of the Earth ($\pm 30^\circ$ latitude) absorbs more energy from the Sun than it radiates back to space. This is illustrated in Figure 1, which shows the annual net radiation for the study year. Note that in this energy excess region, there is considerably more longitudinal variation in the net radiation than there is at higher latitudes where an annual net radiation deficit exists. The energy gradients shown help drive the atmospheric and oceanic currents which carry energy from the excess to the deficit regions. In the atmosphere, the Hadley cells help carry tropical energy to the mid-latitudes. The Walker cell circulation is related to the longitudinal gradients. The ocean currents such as the Pacific Ocean Gyre and the Equatorial Pacific counter current are also important.

The mean annual surface temperatures taken from the Nimbus-7 cloud dataset (Stowe et al., 1988) are shown in Figure 2. Note that there is a general similarity in the net radiation and temperature contours. This is true of both the equator to pole and east-west gradient patterns. Physically, this makes sense since the regions that receive the most heat will generally be the warmest. It helps to simplify the analysis if land and ocean regions are treated separately. To this end, we divide the 2,070 Nimbus-7 ERB target areas into three classes:

Ocean	(over 85% water)
Land	(over 85% land)
Coast	(mixture of land and water)

Figure 3a shows a scatter plot of annual mean net radiation versus surface temperature for the entire globe (2,070 target areas). Two regimes are apparent. The polar regions with mean temperatures below 260°K form a nearly flat tail. In fact there is tendency for the net radiation to decrease as the temperature increases. The polar regions absorb little direct energy from the Sun, thus the OLR is dominant (see Eq.(1)). In this region, the OLR tends to increase, and the net radiation to decrease, as the temperature increases. Over the rest of the globe, where direct solar heating is important, there is a strong correlation between net radiation and surface temperature. Dry continental regions have their own peculiar patterns; notice that the tropical and subtropical Sahara and Arabian deserts (Figure 1) show an annual energy deficit even though the surface temperature is moderately high. In this study, we shall not consider such areas in detail.

Figure 3b treats just the _____ ocean target areas from 45°S to 45°N latitude. The correlation of 95% would seem to explain about 90% of the variance. The major strength in the correlation comes from the equator-to-pole gradients. However, the scatter plot in Figure 4 shows a 76% correlation for the _____ ocean target areas from 4.5°S to 4.5°N latitude. Geographically, the relationship is illustrated in Figure 5. This is an annual mean tropical net radiation map with the surface temperatures $\geq 301^{\circ}\text{K}$ (28°C) or $\leq 297^{\circ}\text{K}$ (24°C) indicated on it. Note that most of the equatorial regions with a mean net radiation over 80 W/m² have mean temperatures of 301°K or greater.

Over the oceans, clouds are a major moderator of albedo and OLR and hence of the net radiation. However, cloud amounts and types are dependent on the local surface temperature and other weather parameters. Thus, clouds can act as a feedback mechanism to increase the net radiant energy to warm regions and decrease it over cool regions. This is shown by the annual net radiation cloud forcing shown

in Figure 6. In the tropics oceans, the warmer regions with mean temperatures of 300°K or greater usually show a low net cloud forcing that may even be positive in nature. These warmer regions tend to have a large percentage of thin cirrus, derived from neighboring deep convective cells, which act to increase the net radiation. On the other hand, the regions with mean temperatures of 297°K or less often are covered by low stratus clouds which produce a strong negative net cloud forcing. Thus, the cool waters along the west coasts of South America and Africa are associated with strong negative cloud forcing, while the warm water in the western Pacific and Indian oceans show patches of positive cloud forcing.

Examining the equator-to-pole gradient, the cold high latitude waters show a strong negative net cloud forcing compared to the relatively mild cloud forcing over the warm tropical waters. Thus, in the mean, cloud feedback related to the surface temperature tends to modulate solar heating to keep warm regions warm and cool regions cool.

Over continents, the variability in the surface water, surface albedo, and the presence of mountains complicate the patterns. However, there are regions such as warm northern India and the cooler South China where the same pattern exists. Our main emphasis in this study is on the oceans.

The analysis, in the next section, of the seasonal variations in the tropics and subtropics yield additional insight on the relationship between clouds, surface temperature, and net radiation.

4. SEASONAL VARIATIONS

The seasonal cycle of the top-of-the-atmosphere insolation is the dominant driving force for the radiation budget. The difference in the seasonal cycle between warm and cool equatorial ocean regions is illustrated in Figure 7 for two ocean target areas in the latitude band (0° to 4.5°S). The monthly mean solar insolation (Figure 7a) is always high with a yearly range of 2 W/m^2 (15%). A minimum, below 400 W/m^2 , occurs in May to June while a prolonged maximum, above 420 W/m^2 , occurs for September to April. The western Pacific rainy region (centered at 2.25°S latitude and 159.75°E longitude) is characterized by plentiful, high clouds and a year-round surface temperature close to 303°K (30°C). Both the net radiation and the cloud amount and altitude increase with the insolation, but the surface temperature shows a slight tendency to decrease during the monsoon peaks.

REFERENCES

- Ardanuy, P. E., H. L. Kyle, and H. D. Chang, 1987: Interannual Observations of the Southern Oscillation: Results from the Nimbus-7 ERB Experiment, *Mon. Wea. Rev.*, **115**, pp. 2615-2625.
- Ardanuy, P. E., C. R. Kondragunta, and H. L. Kyle, 1990: Low-Frequency Modes of the Tropical Radiation Budget, *J. Meteor. and Atmos. Physics*, **44**, 167-194.
- Ardanuy, P. E., L. L. Stowe, A. Gruber, and M. Weiss, 1991: Shortwave, Longwave, and Net Cloud-Radiative Forcing as Determined From Nimbus-7 Observations, *J. Geophys. Res.*, **96**, 18537-18549.
- Arking, A., 1991: The Radiative Effects of Clouds and Their Impact on Climate, *Bull. Amer. Meteor. Soc.*, **71**, 795-813.
- Dhuria, H. L. and H. L. Kyle, 1990: Cloud Types and the Tropical Earth Radiation Budget *J. Climate*, **1990**, 1409-1434.
- Harrison, D. E., 1991: Equatorial Sea Surface Temperature Sensitivity to Net Surface Heat Flux: Some Ocean Circulation Model Results, *J. Climate*, **4**, 539-549.
- Harrison, E. F., P. Minnis, B. R. Barkstrom, V. Ramanathan, R. D. Cess, and G. G. Gibson, 1990: Seasonal Variation of Cloud Radiative Forcing Derived from the Earth Radiation Budget Experiment, *J. Geophys. Res.*, **95**, 18,687-18,703.
- Hartmann, D. L., and D. Doelling, 1991: On the Net Radiative Effectiveness of Clouds, *J. Geophys. Res.*, **96**, 869-891.
- Hartmann, D. L., K. J. Kowalewsky, and M. L. Michelsen, 1991: Diurnal Variations of Outgoing Longwave Radiation and Albedo from ERBE Scanner Data, *J. Climate*, **4**, 598-617.
- Hoyt, V. D., H. L. Kyle, J. R. Hickey, and R. H. Maschhoff, 1991: The Nimbus-7 Total Solar Irradiance: A New Algorithm for its Derivation, *J. Geophys. Res.*, Space Physics, (in press).

Jacobowitz, H., H. V. Soule, H. L. Kyle, F. B. House, et.al., 1984: The Earth Radiation Budget (ERB) Experiment: An Overview, *J. Geophys Res.*, **89**(4), pp. 5021-5038.

Kyle, H. L., Ardanuy, P. E., and E. J. Hurley, 1985: The Status of the Nimbus-7 ERB Earth Radiation Budget Data Set, *Bull. Amer. Meteor. Soc.*, **66**, pp. 1378-1388.

Lewis, M. R., M. Carr, G. C. Feldman, W. Esaias, and C. McClain, 1990: Influence of Penetrating Solar Radiation on the Heat Budget of the Equatorial Pacific Ocean, *Nature*, **347**, 543-545.

Platt, C. M. R., 1981: The Effect of Cirrus of Varying Optical Depth on the Extraterrestrial Net Radiative Flux, *Quart. J. Roy. Meteor. Soc.*, **107**, 671-678.

Prabhakara, C., R. S. Fraser, G. Dalu, M. C. Wu, and R. J. Curran, 1988: Thin Cirrus Clouds: Seasonal Distribution Over Oceans Deduced from Nimbus-4 IRIS, *J. Appl. Meteor.*, **27**, 374-399.

Ramanathan, V., 1987: The Role of Earth Radiation Budget Studies in Climate and General Circulation Research, *J. Geophys. Res.*, **92**(4), pp. 4075-4095.

Ramanathan, V. and W. Collins, 1991: Thermodynamic Regulation of Ocean Warming by Cirrus Clouds Deduced From Observations of the 1987 El Niño, *Nature*, **351**, 27-32.

Ramanathan, V., R. D. Cess, E. F. Harrison, P. Minnis, B. R. Barkstrom, E. Ahmad, and D. Hartmann, 1989: Cloud-Radiative Forcing and Climate: Results From the Earth Radiation Budget Experiment, *Science*, **243**, 57-63.

Stephens, G. L., 1990: On the Relationship Between Water Vapor Over the Oceans and Sea Surface Temperature, *J. Climate*, **3**, 634-645.

Stowe, L. L., C. G. Wellemeyer, T. F. Eck, H. Y. M. Yeh, and the Nimbus-7 Cloud Data Processing Team, 1988: Nimbus-7 Global Cloud Climatology, Part I: Algorithms and Validation, *J. Climate*, **1**, pp. 445-470.

Stowe, L. L., H. Y. M. Yeh, T. F. Eck, C. G. Wellemeyer, H. L. Kyle, and the Nimbus-7 Cloud Data Processing Team, 1989: Nimbus-7 Global Cloud Climatology, Part II: First Year Results, *J. Climate*, **2**, pp. 671-709.

Wielicki, B. A. and R. N. Green, 1989: Cloud Identification for ERBE Radiative Flux Retrieval, *J. Appl. Meteor.*, **28**, pp. 1131-1146.

FIGURE CAPTIONS

- Figure 1. The annual net radiation observed by the Nimbus-7 ERB scanner for the year June 1979 to May 1980. The units are W/m^2 and the contour intervals is 20 W/m^2 .
- Figure 2. The annual net radiation cloud forcing observed by the Nimbus-7 ERB scanner. The contour step is 15 W/m^2 . The dots indicate regions with insufficient cloud-free observations.
- Figure 3. The tropical annual net radiation and its relation to the surface temperature are shown. Shadings rising from left to right indicate regions where the mean annual temperature is greater than or equal to 301°K . Shadings declining from left to right show regions where the mean temperature is less than or equal to 297°K .
- Figure 4. A scatter plot of mean annual sea-surface temperature versus annual net radiation for the equatorial ocean ($\pm 4.5^\circ$ latitude) is shown for the year June 1979 to May 1980. The data are from the Nimbus-7 ERB and cloud datasets. Each square represents one of the 111 $(500 \text{ km})^2$ ocean target areas along the equator.

NIMBUS-7 MLCE NET RADIATION JUNE 79-MAY 80

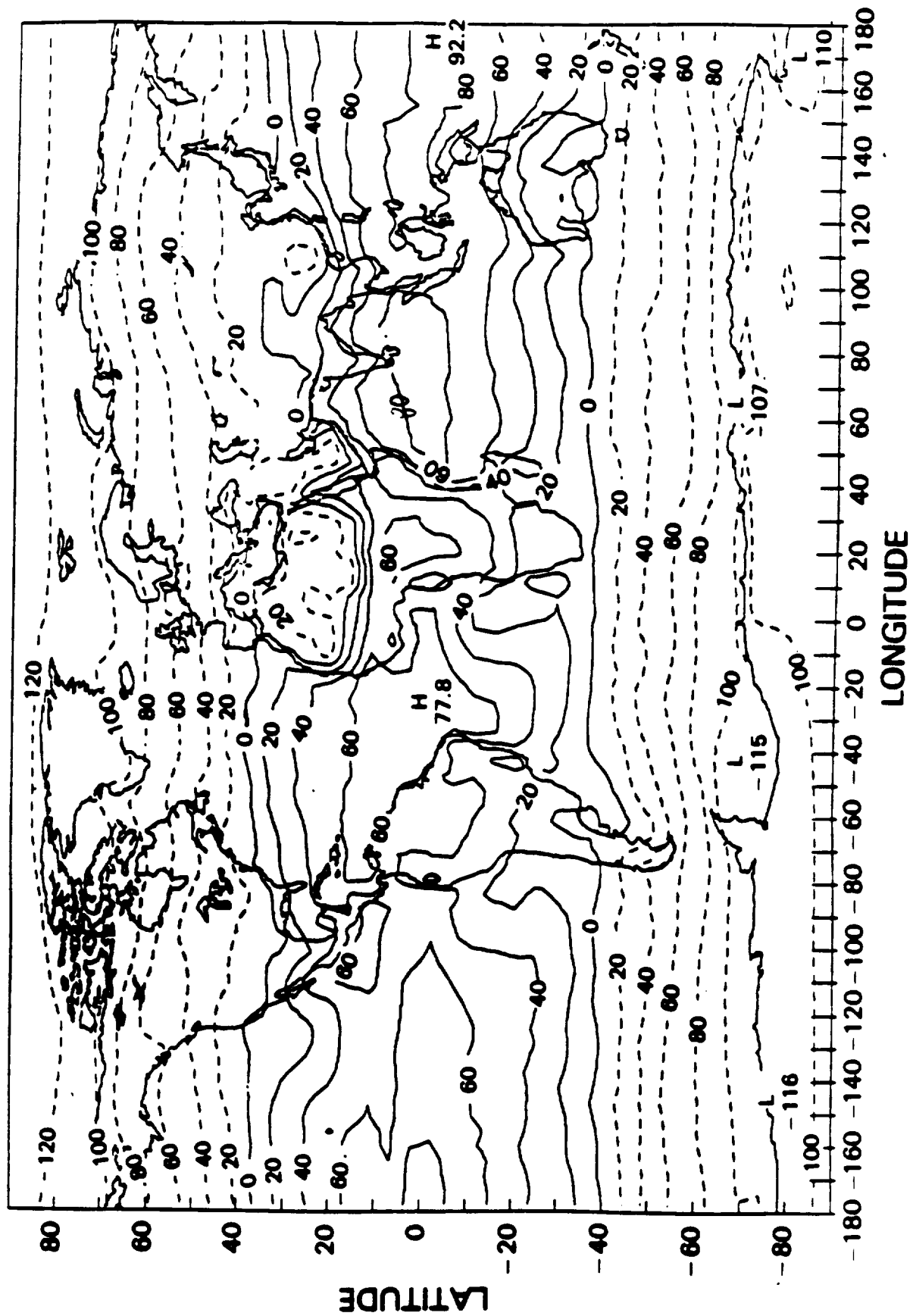


Fig. 1

NIMBUS 7/NET CLOUD FORCING (W/M-M) JUNE 1979 - MAY 1980

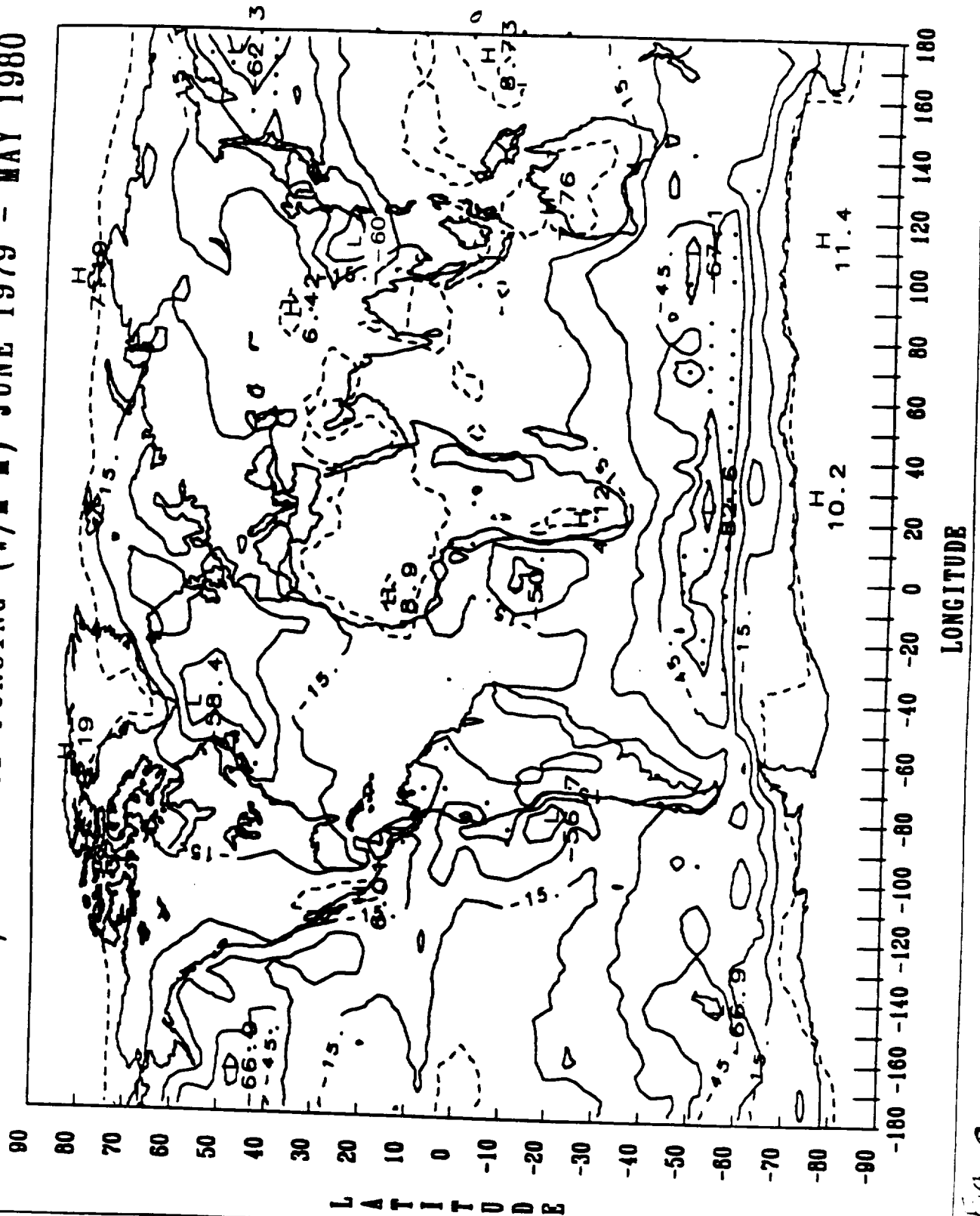


Fig. 2

NET RADIATION — JUNE 1979 - MAY 1980

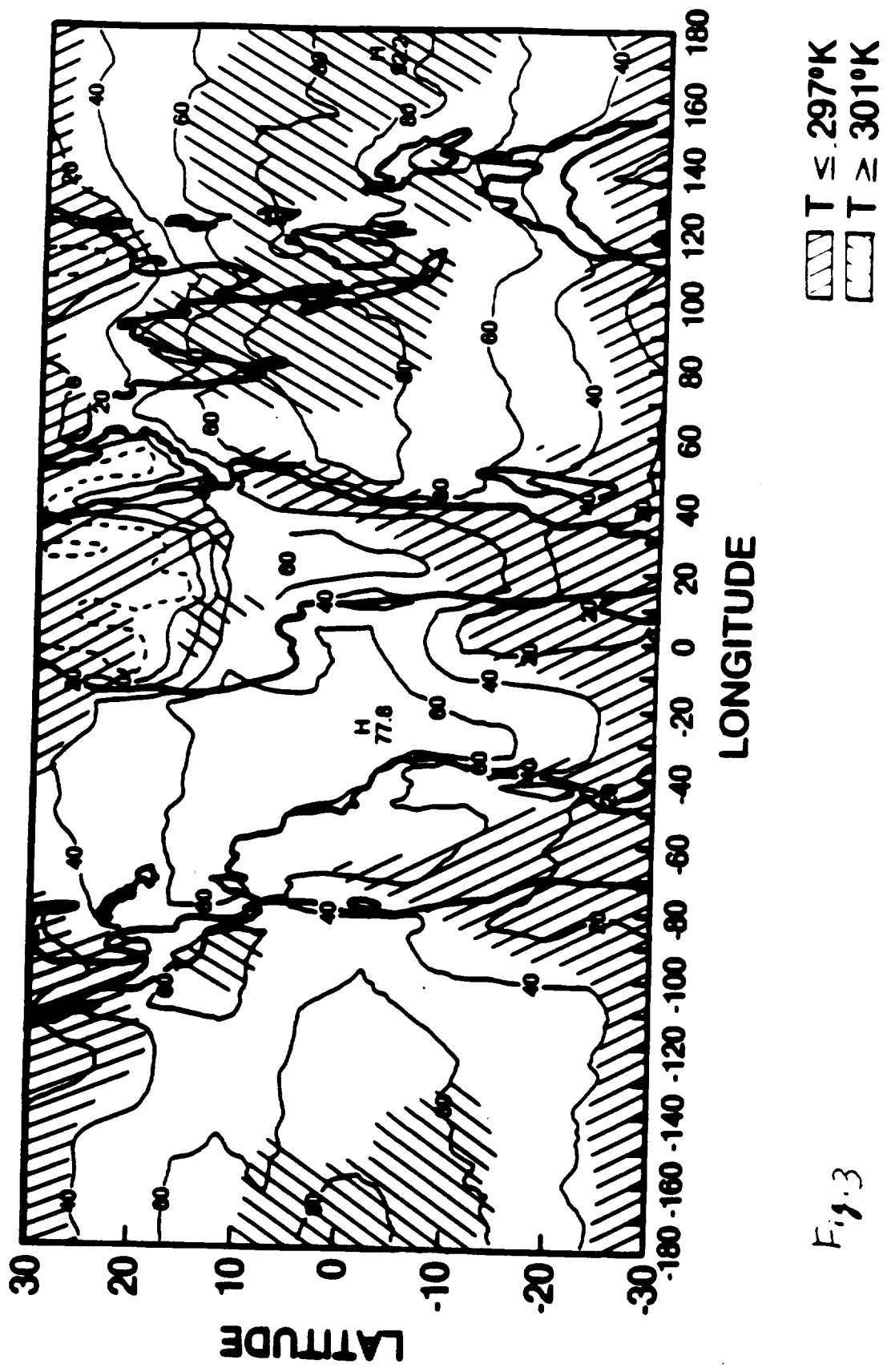


Fig. 3

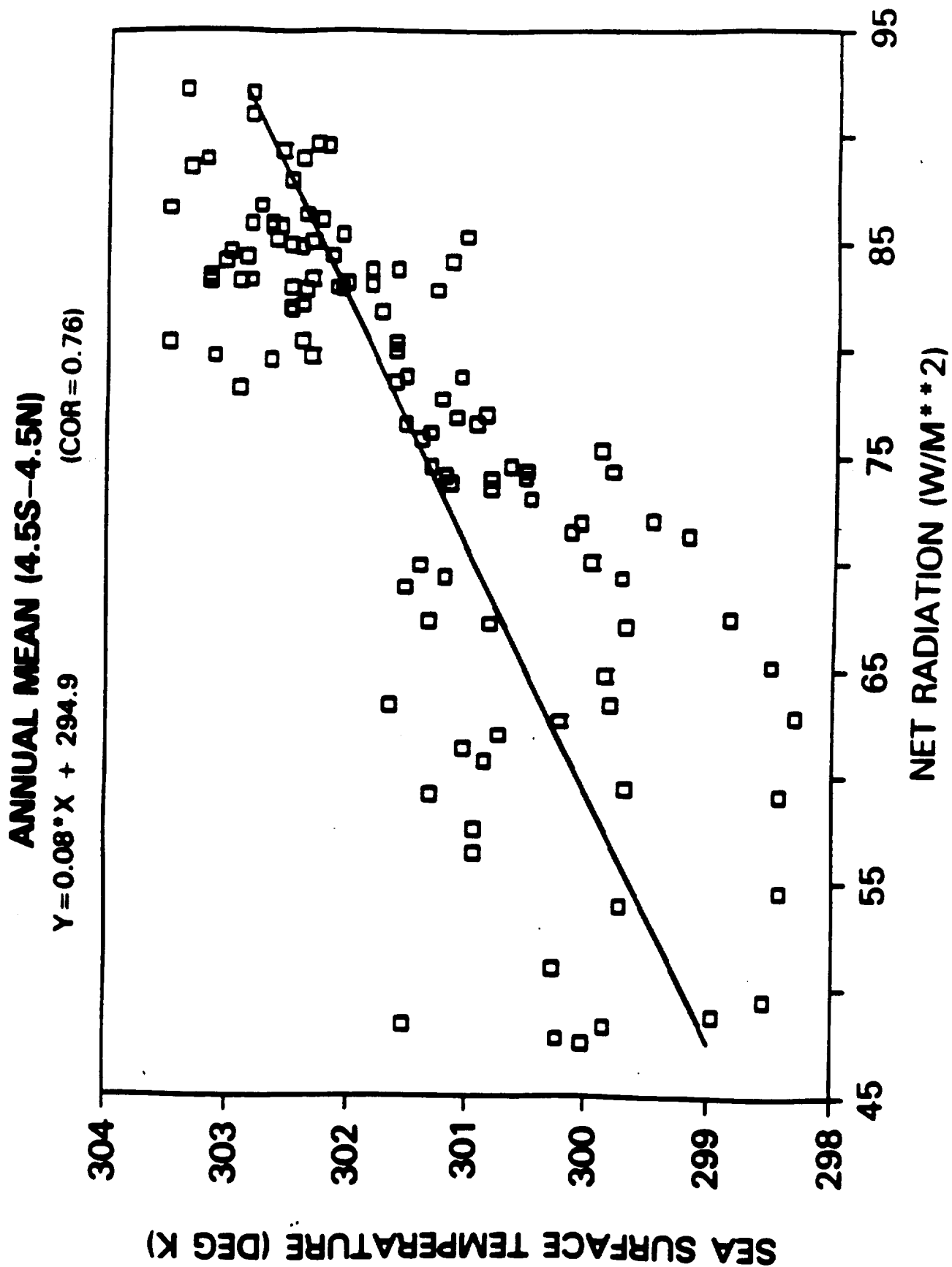


Fig. 4

SEA-SURFACE TEMPERATURE AND THE SOLAR IRRADIANCE IN THE TROPICS

Harbans L. Dhuria (University of the District of Columbia, Washington, DC
20008, USA)

H. Lee Kyle (NASA/Goddard Space Flight Center, Greenbelt, MD 20771, USA)

1992 SPRING MEETING

May 13, 1992

MONTREAL
May 12-16, 1992

American Geophysical Union

SUMMARY

Examination of one year (June 1979 to May 1980) of Nimbus-7 Earth Radiation Budget (ERB) and Cloud Data reveals a correlation of about 0.85 between the mean annual equatorial sea-surface temperature (SST) and the net radiation. This seems reasonable: the greater the energy absorbed from the Sun, the higher the temperature should be. However, closer study suggests that the SST acts in a mean fashion to control the net radiation with cloud type and amount serving as the control mechanism. The equatorial Pacific is the prime example. The warm water pool in the west has a relatively constant temperature at or above 28°C during this whole year. It has both heavy, deep convective cloud cover and a high net radiation that averages over 85 W/m². The cloud-induced decrease in the absorbed solar radiation is compensated by the decrease in the top of the atmosphere (TOA)-emitted

longwave radiation. This region is the source of both Walker and Hadley cell atmospheric circulation cells and exports a large amount of energy both to higher latitudes and to other tropical regions. In this region when the SST climbs to 30°C or above, the albedo increases as the clouds thicken and both the net radiation and SST decrease somewhat. The cool water sector along the west coast of South America behaves very differently. Here the mean SST is about 25.5° with a seasonal range of 23°C to 27°C and low stratus clouds strongly reduce the net radiation. The cloud amount varies inversely, and the net radiation and SST vary directly with the solar irradiance. Thus, the SST and net radiation peak in February and March as does the absorbed solar irradiance. During these months, SST and net radiation are high over most of the tropical oceans and the correlation breaks down. The east central equatorial Pacific is normally a high pressure region with low to moderate cloud cover and SST mostly in the 26°C to 27°C range. Both the absorbed shortwave and emitted longwave are high, thus, the resultant net radiation is normally intermediate between the regions to the east and west of it. In an El Niño year, there will, of course, be regional variations in the pattern described here. Globally there is a strong correlation between annual averages of insolation, net radiation, and SST. The controlling factor is undoubtedly the equator-to-pole variation in the insolation. The correlation breaks down in the summer hemisphere when the TOA insolation is high over the entire hemisphere.

DATA SOURCES

The Nimbus-7 ERB scanner products (Jacobowitz, et al., 1984; Ardanuy et al., 1990) and the Nimbus-7 cloud products (Stowe et al., 1989) were used in this study. The

cloud products include the Air Force 3-D Neph-Analysis SST data. Monthly averages over (4.5° latitude by 4.5° longitude) regions were used. Diurnal averages of the emitted longwave, absorbed shortwave and net radiation, and of the SST were used together with the nighttime cloud observations. This study concentrates on the equatorial belt from 4.5°S to 4.5°N latitude. In this belt, there are 160 regions of which 113 are ocean regions (55 S and 58 N of the equator).

THE EARTH RADIATION BUDGET

The net Earth radiation (NR) is given by

$$\begin{aligned}
 \text{NR} &= (1-A)I_s - F(\text{LW}). & (1) \\
 &= \text{absorbed} - \text{emitted.} \\
 A &= \text{diurnally averaged albedo.} \\
 I_s &= \text{diurnally averaged (solar) insolation.} \\
 F(\text{LW}) &= \text{diurnally averaged outgoing longwave radiation (OLR).}
 \end{aligned}$$

The measured quantities are the reflected shortwave $F(\text{SW})$, the emitted longwave, and the solar irradiance. The albedo and $F(\text{SW})$ are related by

$$F(\text{SW}) = AI_s. \quad (2)$$

Both the albedo and OLR are strongly influenced by clouds.

The effect of the clouds on the radiation parameters is often discussed as cloud forcing (CF) terms (Ramanathan, 1987), where

$$CF = F(\text{clear}) - F(\text{average}). \quad (3)$$

$F(\text{clear})$ = clear-sky flux.

$F(\text{average})$ = mean observed flux also called the all-sky value.

and

$$CF(\text{NR}) = CF(\text{SW}) + CF(\text{LW}).$$

The shortwave forcing, $CF(\text{SW})$, is almost always negative, while the longwave forcing, $CF(\text{LW})$, is generally positive.

DISCUSSION

Our ongoing study examines the relationship between the Earth's Radiation Budget (ERB) and the Tropical Sea Surface Temperature (SST). This is a preliminary report. The Earth's climate is dominated by the fact that the mean annual, top of the atmosphere (TOA) insolation is over twice as large in the tropics as in the Polar regions. In addition, a higher percentage of incident solar irradiance is absorbed at low latitudes (Fig. 1). As a result, excess heat is absorbed from the Sun in the tropics and transported by ocean and atmosphere currents to the high latitudes. In the global annual mean, the TOA insolation, net radiation, and SST are closely coupled. The scatter plot in Fig. 2 shows the net radiation/SST annual mean

relationship. This relationship is basically governed by the equator-to-Pole gradient in the insolation. The TOA insolation is high over the entire summer hemisphere (see Fig. 3) and the net radiation/SST relationship becomes quite weak (Fig. 4). In the winter hemisphere, it remains strong (Fig. 5).

A similar relationship exists between the net radiation and SST along the Equator (Figs. 6 and 7). However, here the TOA insolation is always relatively high, and neither the net radiation nor the SST appears closely linked to the quantity of absorbed solar radiation. Our supposition is that the equatorial SST is more strongly controlled by ocean conditions (see for instance Philander, 1989) than by the absorbed solar radiation.

The equatorial ocean monthly zonal means are given in Table 1 for the TOA insolation, net radiation (NR) SST and the (NR/SST) spectral correlation. The annual averages are at the bottom; however, the annual correlation refers to correlation of the annual averages. Regional differences are accentuated in the annual means and, thus, the annual correlations are larger than the monthly values. When the two zones are combined (Fig. 6), the correlation of the annual means decreases somewhat. This may be related to the zonal difference in the mean net radiation (Table 1).

The seasonal variations in two ocean regions just south of the equator are illustrated in Figs. 8A and B. One region is just north of New Guinea in the western Pacific, warm water, equatorial rain belt. The other is in the cool water Eastern Pacific just off the coast of South America. Both receive the same TOA insolation but the

results are quite different. The Western Pacific region always has a high SST and a heavy but variable cloud cover. Interestingly, the SST at times decreases slightly when the insolation is high. These decreases seem associated with slight decreases in the net radiation (Fig. 8A) and slightly negative net cloud forcing (Fig. 8B). Thus, as Ramanathan and Collins (1991) suggested, clouds appear to act as a control to keep the SST from exceeding a value of 32°C.

The Eastern Pacific region has a low stratus cloud cover which decreases the net radiation in the June to October period. However, this cloud cover decreases sharply in the January to May period and the net radiation increases sharply (Fig. 8A). There is an associated rise in the SST.

CONCLUSIONS

There is a strong correlation of about 0.85 between the mean annual SST and the net radiation over the Equatorial Ocean. This correlation appears to be due to associated regional differences in SST and cloud cover. Cirrus clouds associated with deep convective activity and warm SST increase the net radiation. On the other hand, low stratus clouds, associated with cool SST decrease the net radiation (see for instance Dhuria and Kyle, 1990). The SST itself appears to be principally controlled by ocean and atmosphere circulation patterns (see for instance Philander, 1989). However, insolation and cloud changes do appear to have some influence on the +SST. This correlation refers to an overall pattern of conditions and it does not hold equally true in all time periods.

REFERENCES

- Ardanuy, P. E., C. R. Kondragunta, and H. L. Kyle, 1990: Low-Frequency Modes of the Tropical Radiation Budget, *J. Meteor. and Atmos. Physics*, **44**, 167-194.
- Dhuria, H. L., and H. L. Kyle, 1990: Cloud Types and the Tropical Earth Radiation Budget, *J. Climate*, **3**, 1409-1434.
- Jacobowitz, H., H. V. Soule, H. L. Kyle, F. B. House, and the ERB Nimbus-7 Experiment Team, 1984: The Earth Radiation Budget (ERB) Experiment: An Overview, *J. Geophys Res.*, **89**(4), 5021-5038.
- Philander, G., 1989: El Niño and La Niña, *American Scientist*, **77**, 451-549.
- Ramanathan, V., 1987: The Role of Earth Radiation Budget Studies in Climate and General Circulation Research, *J. Geophys. Res.*, **92**(4), 4075-4095.
- Ramanathan, V., and W. Collins, 1991: Thermodynamic Regulation of Ocean Warming by Cirrus Clouds Deduced from Observations of the 1987 El Niño, *Nature*, **351**, 27-32.
- Stowe, L. L., H. Y. M. Yeh, T. F. Eck, C. G. Wellemeyer, H. L. Kyle, and the Nimbus-7 Cloud Data Processing Team, 1989: Nimbus-7 Global Cloud Climatology, Part II: First Year Results, *J. Climate*, **2**, pp. 671-709.

TABLE 1. ZONAL MEAN EQUATORIAL OCEAN SEASONAL VARIATIONS

MONTH/ YEAR	4.5°S to 0° (No. = 55)					0° to 4.5°N (No. = 58)				
	I _s (W/m ²)	NR (W/m ²)	SST (°K)	NR/SST Correlation	I _s (W/m ²)	NR (W/m ²)	SST (°K)	NR/SST Correlation		
6/79	379.0	41.70	300.78	0.75	394.4	53.76	300.87	0.84		
7/79	384.3	44.92	300.35	0.77	403.1	59.76	300.34	0.79		
8/79	406.4	60.84	299.72	0.66	419.0	74.04	300.27	0.72		
9/79	428.8	81.63	299.74	0.75	431.6	83.82	300.36	0.80		
10/79	437.4	87.10	299.95	0.67	429.3	83.49	300.59	0.71		
11/79	431.9	84.23	300.17	0.66	414.8	68.38	300.65	0.71		
12/79	425.4	80.72	300.35	0.70	403.8	56.65	300.65	0.76		
01/80	430.9	92.26	300.45	0.73	411.2	63.33	300.37	0.81		
02/80	441.4	99.73	300.61	0.39	429.2	77.18	300.87	0.68		
03/80	440.3	97.61	300.85	0.26	438.7	86.44	300.87	0.68		
04/80	421.3	87.09	301.02	0.26	430.5	84.22	301.20	0.59		
05/80	395.0	61.83	301.28	0.69	412.0	70.03	301.41	0.75		
Annual Average	418.52	76.65	300.44	0.84(a)	418.4	71.76	300.68	0.87(a)		

I_s = Top of the Atmosphere Solar Irradiance (Insolation)

NR = Net Radiation

SST = Sea Surface Temperature

No. = Number of Ocean Regions in the Zone

(a) = Correlation of the Annual Means

ZONAL AVERAGES (ANNUAL)

Nimbus-7 (All Sky)

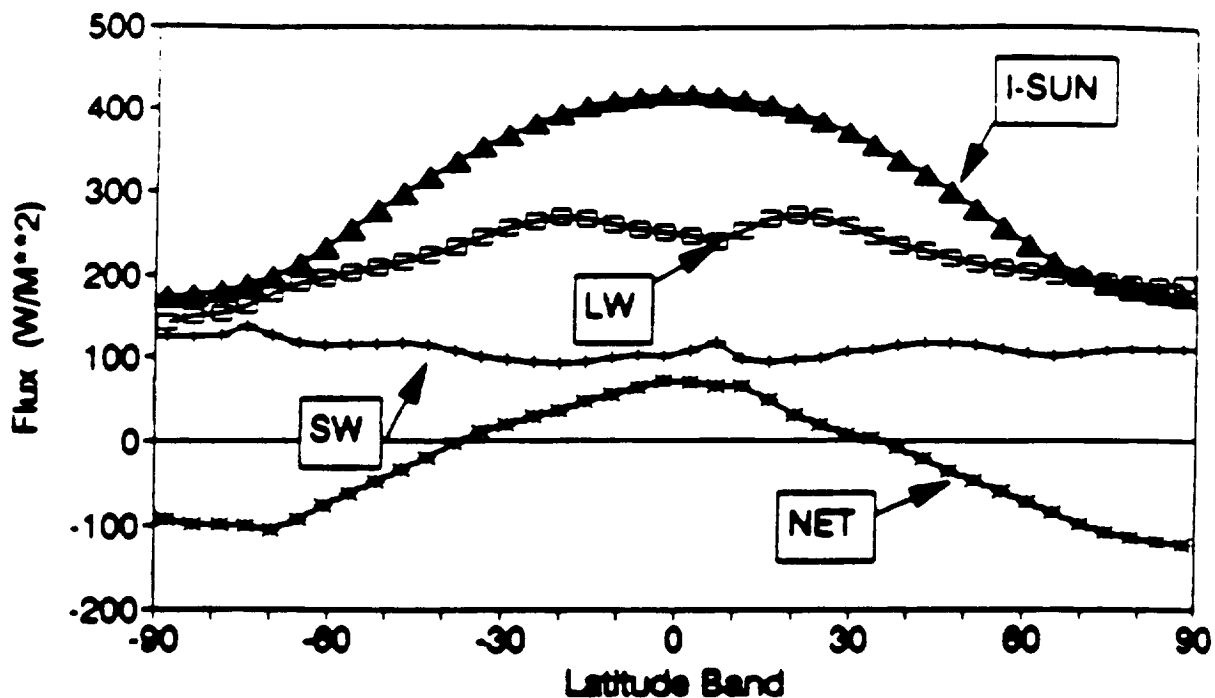


Figure 1. Nimbus-7 scanner (MLCE) annually and zonally averaged (June 1979 through May 1980) emitted longwave (LW), reflected shortwave (SW), net radiation (NR), and top-of-the-atmosphere insolation, I(sun).

TABLE 1

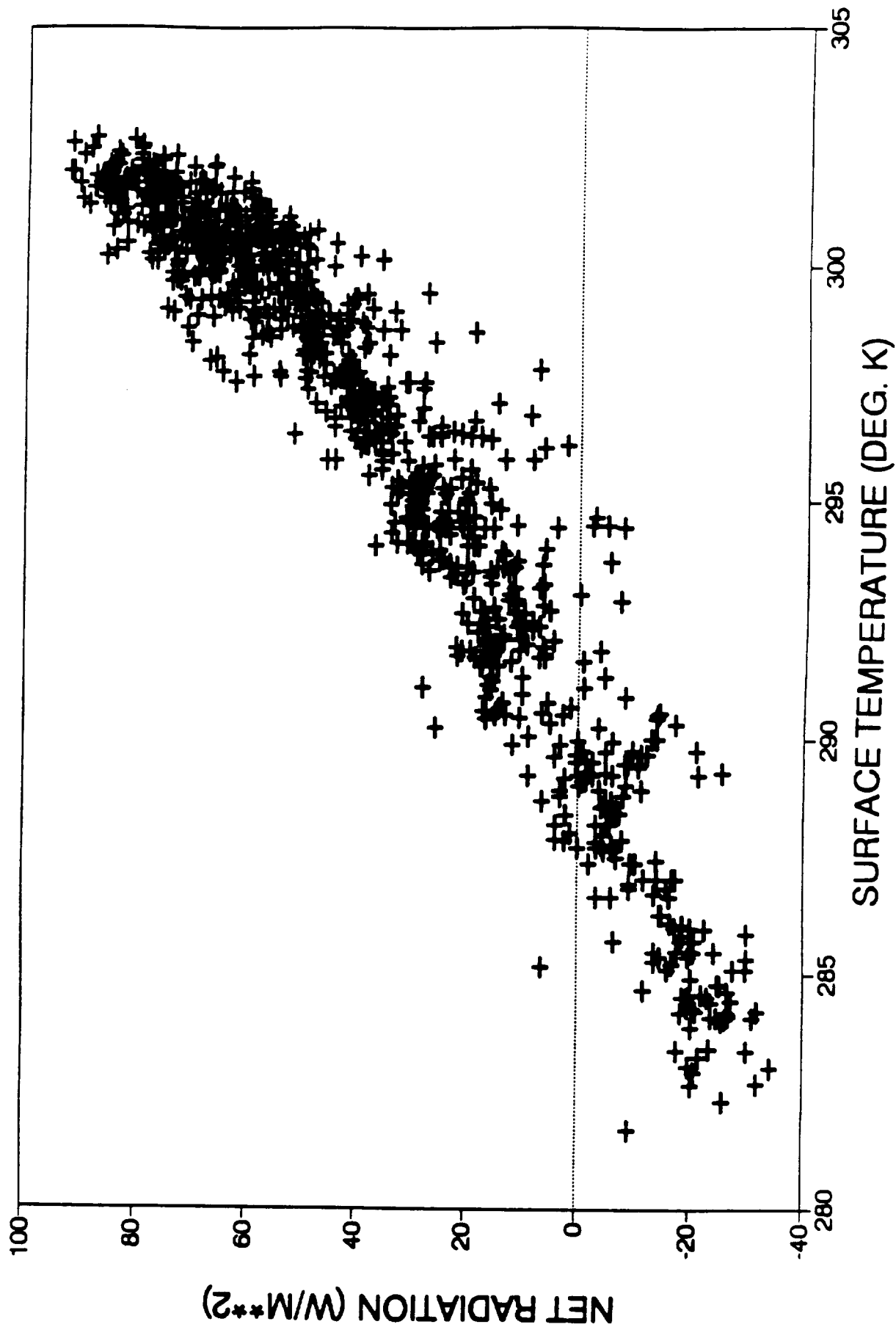
JULY 1979 TROPICAL OCEAN REGIONS (LAND EXCLUDED)
CORRELATION COEFFICIENTS OF NET RADIATION WITH

REGION	LAT	LO	OLR	ALBEDO	DAY	NIGHT	TOTAL CLOUD
NORTHERN MONSOON							
1. PACIFIC	(0-18°N)	(167.5-180°E)	0.319	-0.776	-0.183	-0.042	-0.042
2. PACIFIC	(0-18°N)	(135-167.5°E)	0.525	-0.875	-0.575	-0.244	-0.244
3. PHILLIPINES	(0-22.5°N)	(112.5-135°E)	0.565	-0.861	-0.569	-0.270	-0.270
4. BAY OF BENGAL	(0-22.5°N)	(81-112.5°E)	0.482	-0.859	-0.511	-0.185	-0.185
5. INDIAN OCEAN	(0-22.5°N)	(58.5-81°E)	0.148	-0.749	-0.438	0.079	0.079
SOUTHERN TROPICS							
6. S. AM. COAST	(0-31.5°S)	(72-90°W)	0.020	-0.758	-0.319	-0.059	-0.059
7. PACIFIC	(0-18°S)	(90-112.5°W)	0.018	-0.812	-0.655	-0.369	-0.369
8. PACIFIC	(0-18°S)	(112.5-135°W)	-0.122	-0.689	-0.575	-0.239	-0.239
9. PACIFIC	(0-18°S)	(135-167.5°W)	0.193	-0.679	-0.591	-0.224	-0.224
10. PACIFIC	(0-18°S)	(167.5-180°W)	0.160	-0.695	-0.579	-0.241	-0.241

$R^2 = 0.9$

NET RAD (VS) SURFACE TEMP. (OCEAN)

JUN '79 - MAY '80 (45S - 45N) $R^2 = 0.95$



ZONAL AVERAGES (JJA)

Nimbus-7 (All Sky)

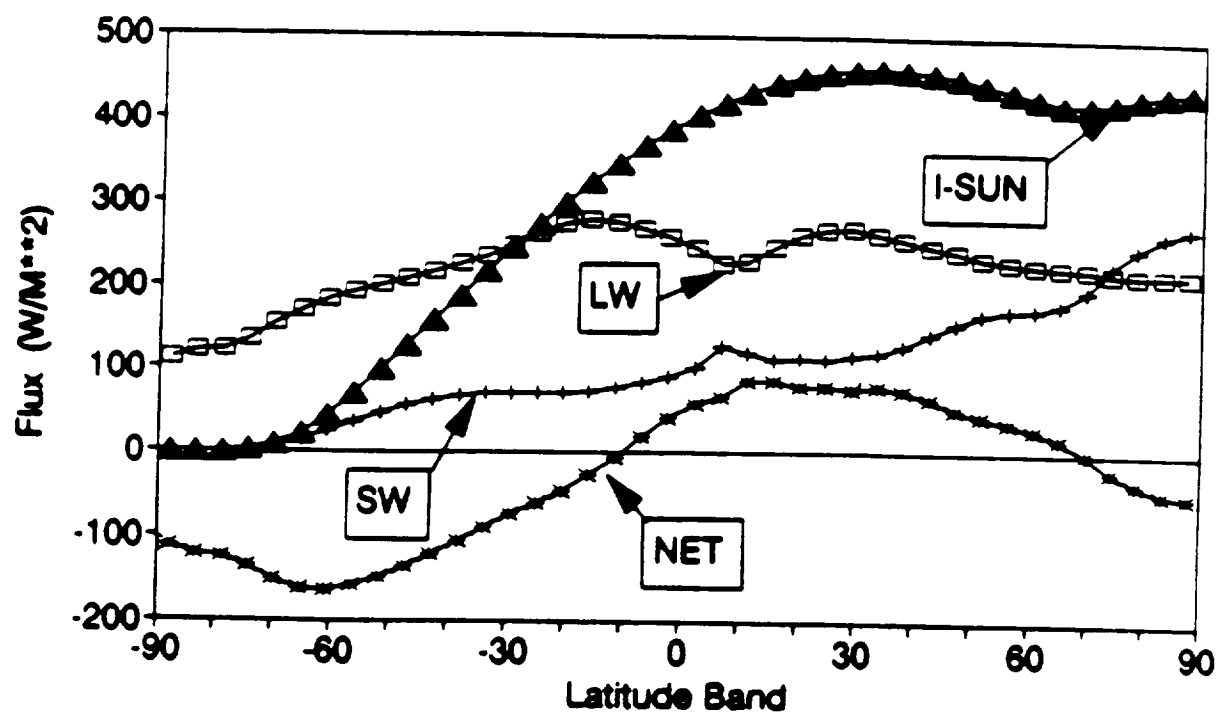
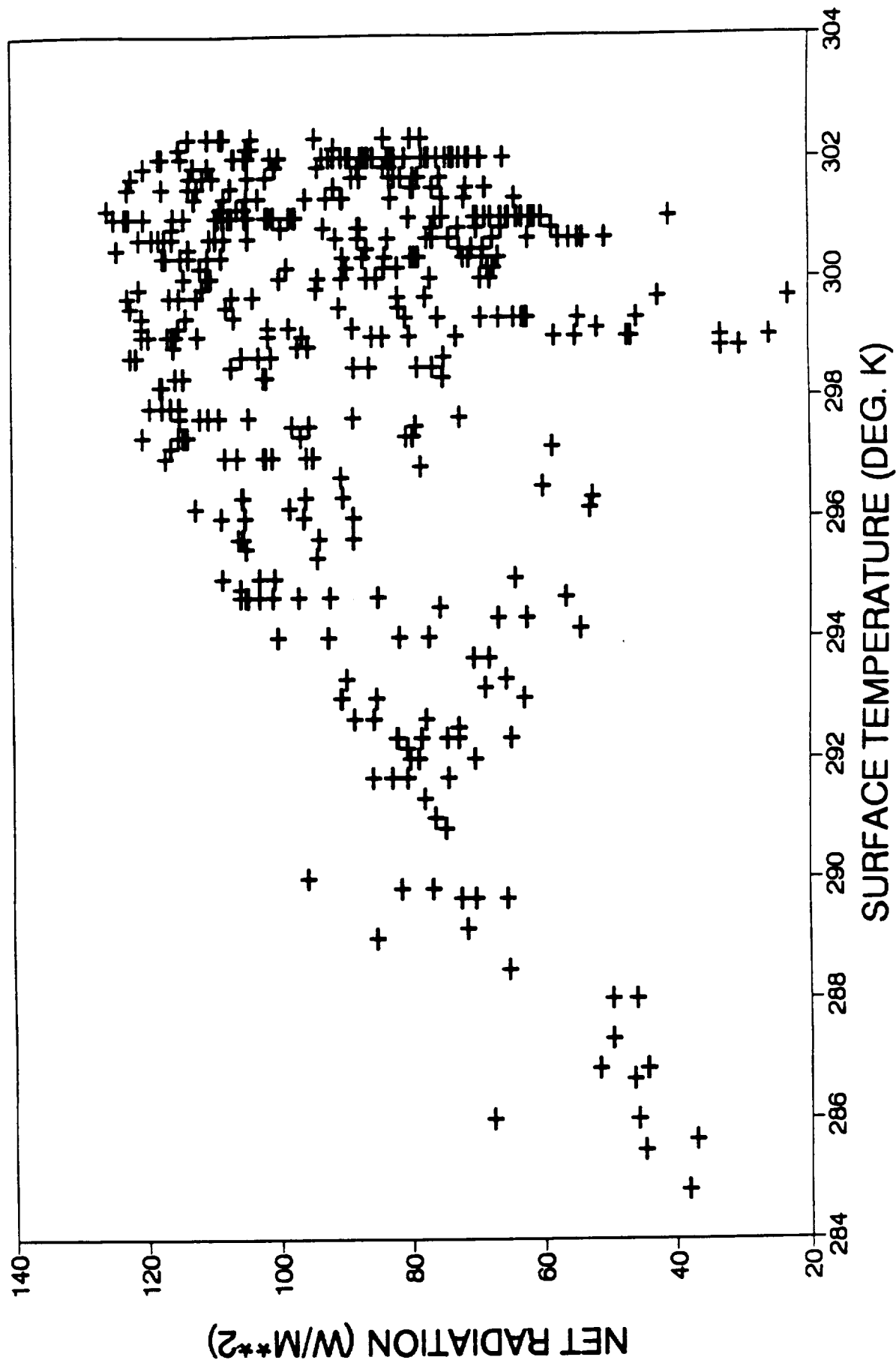


Figure 3. Zonally averaged Earth radiation budget parameters for June 1979 through August 1979 (see Figure 1).

$R^2 \approx 0.07$

NET RAD (VS) SURFACE TEMP. (OCEAN)

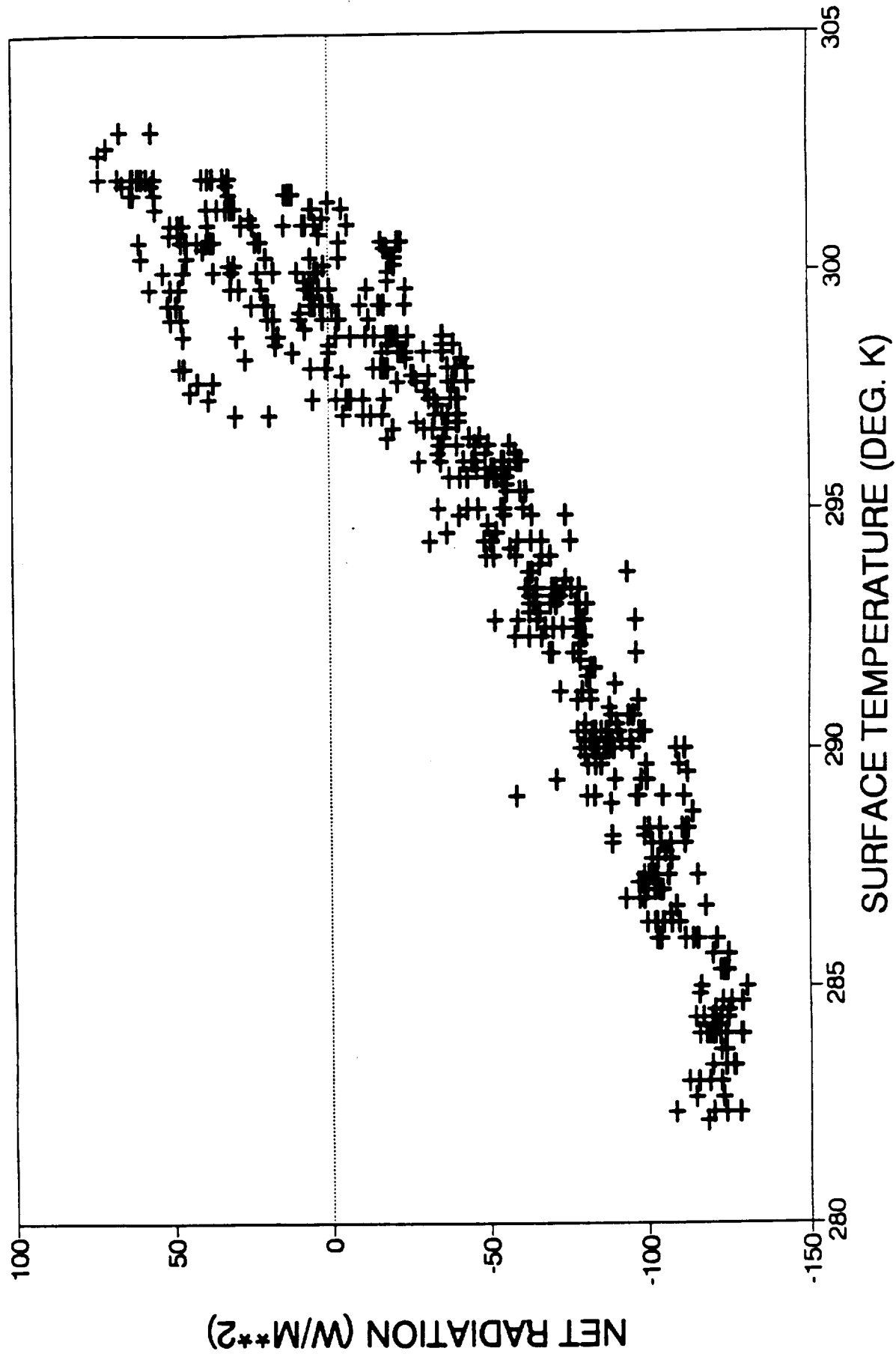
JUN '79 - AUG '79 (EQ - 45N) $R \approx 0.26$



$R^2 = 0.86$

NET RAD (VS) SURFACE TEMP. (OCEAN)

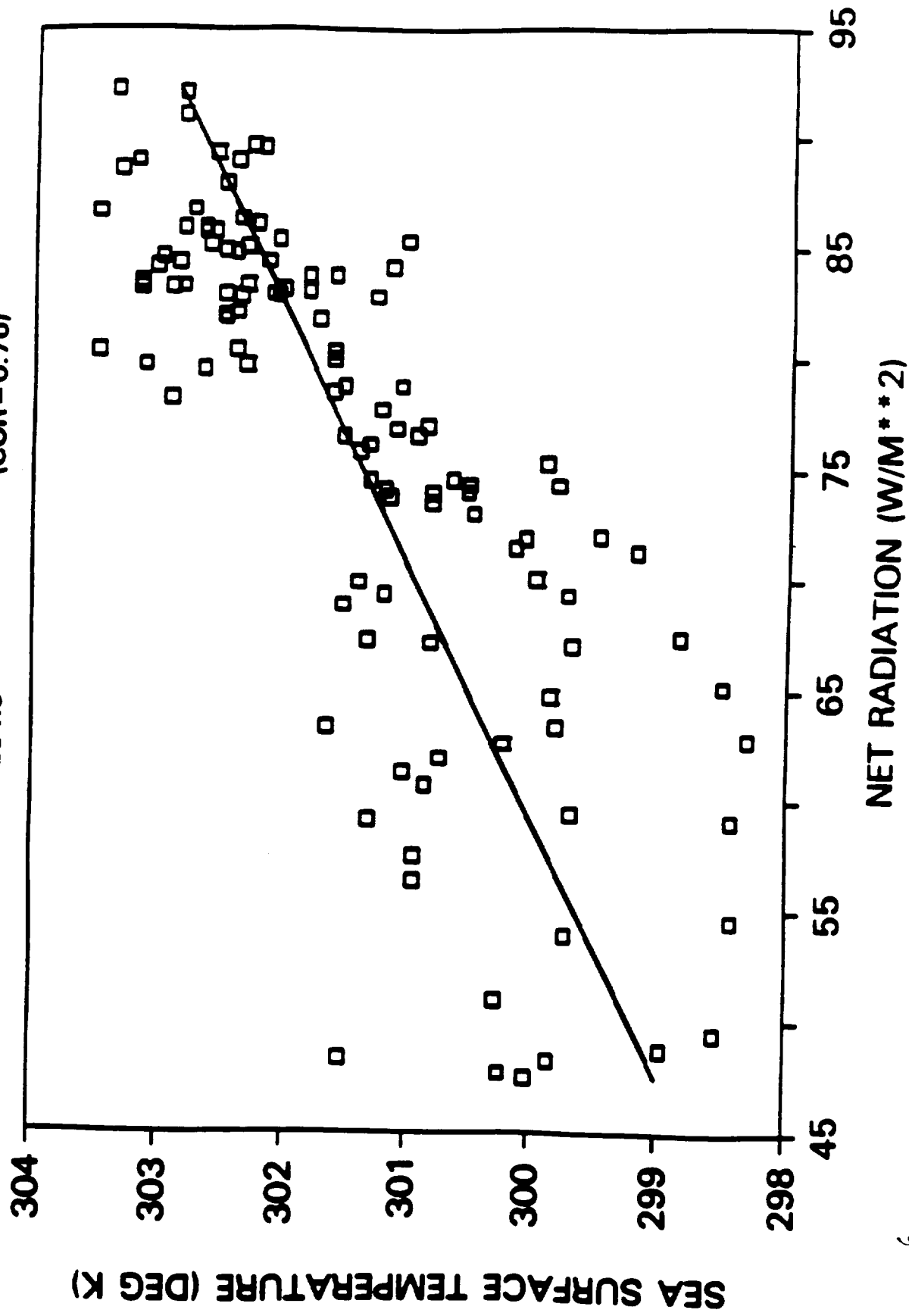
JUN '79 - AUG '79 (45S - EQ) $R = 0.93$



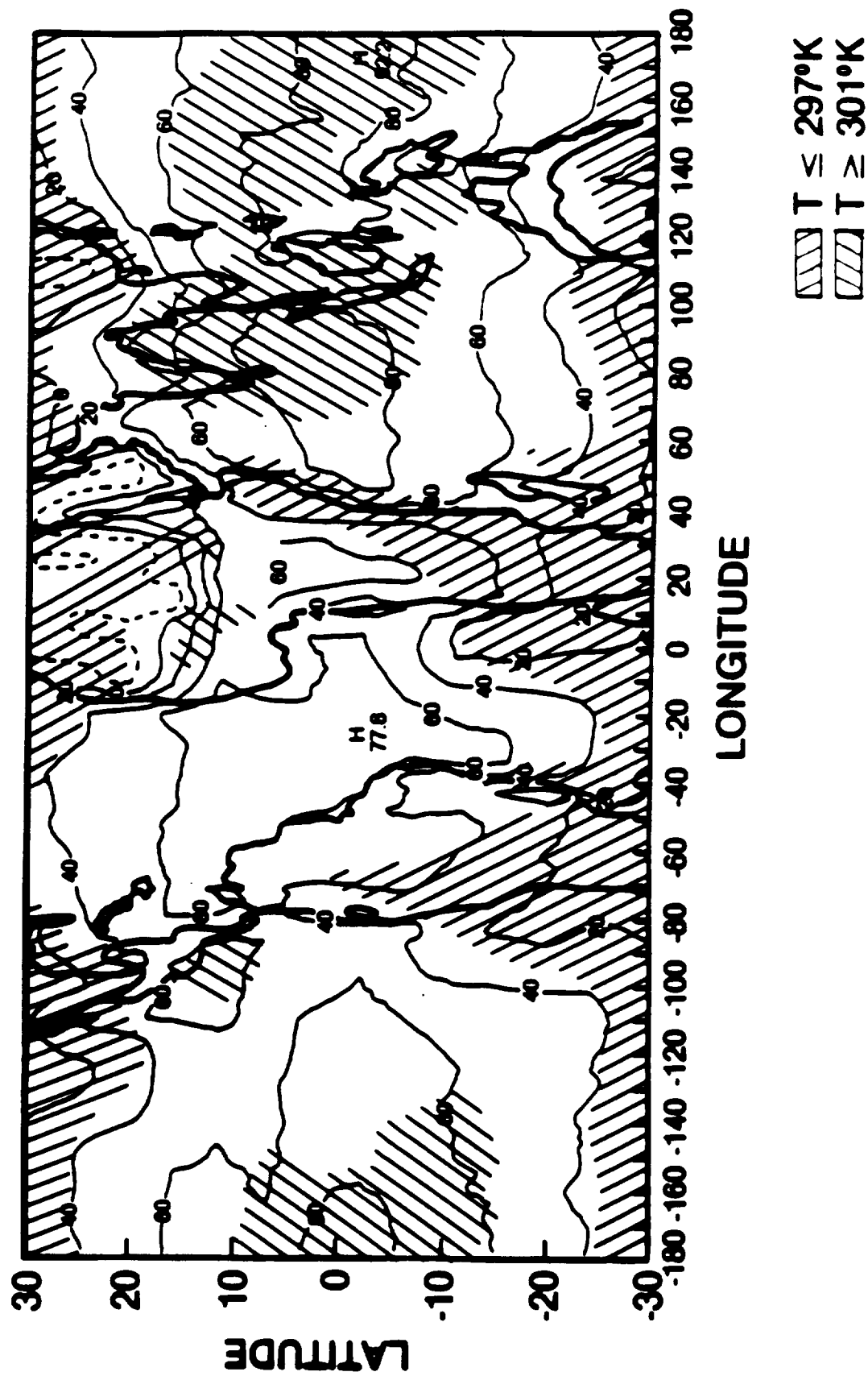
ANNUAL MEAN (4.5S-4.5N)

$$Y = 0.08 * X + 294.9$$

(COR = 0.76)

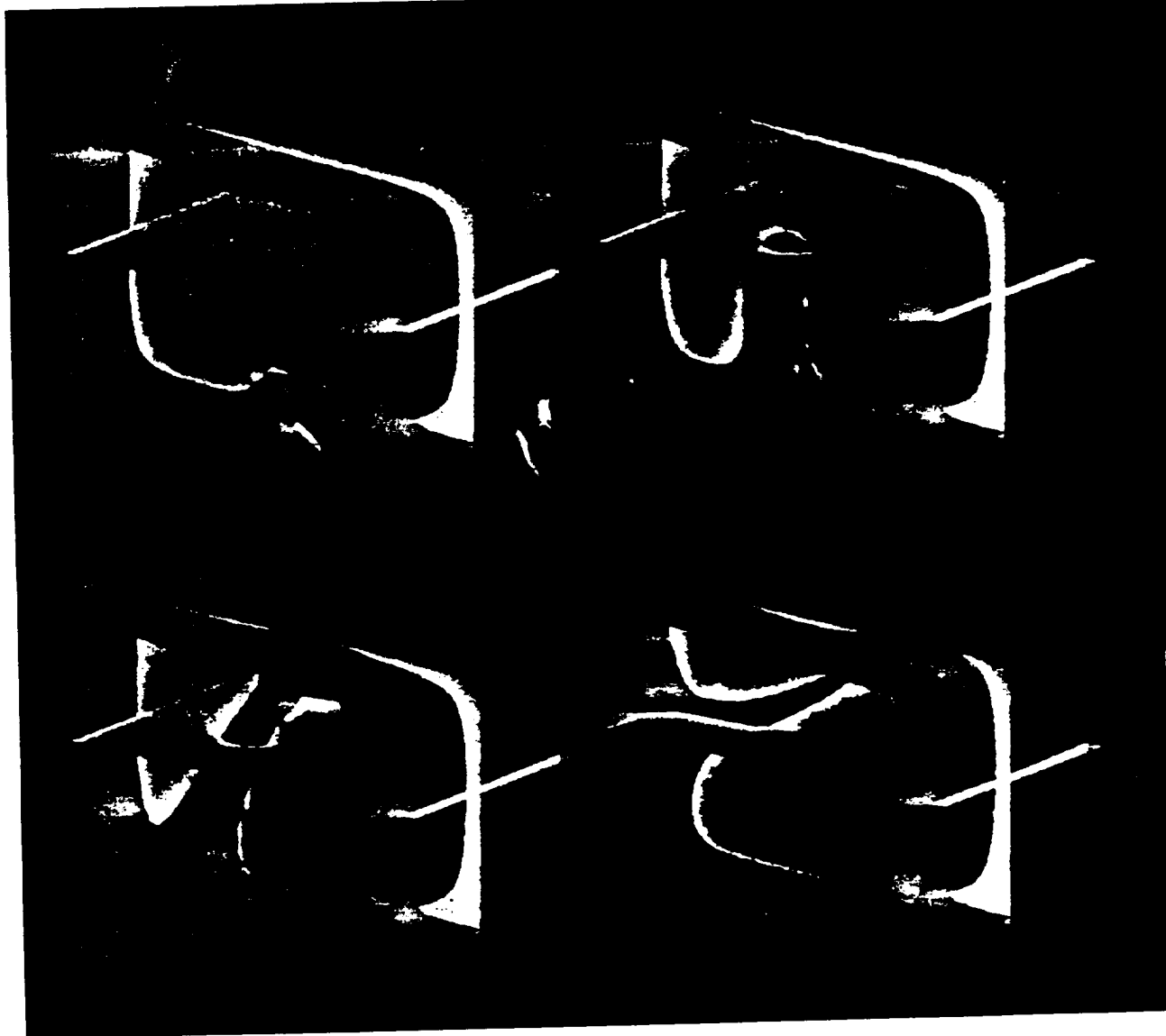


NET RADIATION — JUNE 1979 · MAY 1980



1992 SPRING MEETING

American Geophysical Union
Canadian Geophysical Union
Mineralogical Society of America



Published as a supplement to *Eos*, April 7, 1992

MONTREAL
May 12-16, 1992

Unclass

0136196 N93-18870

(NASA-CR-191619) EFFECTS OF CLOUDS ON THE EARTH RADIATION
BUDGET: SEASONAL AND INTER-ANNUAL PATTERNS Ann... Harbans L.
Dhuria (District of Columbia Univ.) 24 Dec. 1992 44 p
NAS 1.26:191619

G3
E
45

1992 SPRING MEETING

American Geophysical Union ■ Canadian Geophysical Union
Mineralogical Society of America
May 12–16, 1992 Montreal, Canada

Cover: Earth's mantle, the region of solid but viscously deformable rock between the surface and a depth of approximately 3000 km, is vigorously convecting. The most obvious surface manifestations of convection are subduction zones and seafloor spreading. This figure examines the development of a mantle plume, a concentrated area of hot upwelling material believed to be responsible for hotspots such as the Hawaiian island chain.

This three-dimensional numerical model tracks the development of thermal instabilities at the base of an already convecting mantle and the interaction of the resulting plume with the larger scale mantle circulation associated with plate tectonics. In the calculation depicted, we capture the three-dimensional nature of assumed whole-mantle convection but simplify the geometry using a rectangular box with stress-free and insulating side boundaries. The calculation is visualized with two semi-transparent surfaces of constant temperature (red, hot; blue, cold) and two slices, one vertical and one horizontal, where color varies according to the temperature of the slice. The temperature of the convecting fluid is plotted at four time intervals scaled to approximately 20 million years between frames.

The calculation begins with a convection roll (top left frame) upwelling hot fluid on the left and downwelling cold fluid on the right. As the calculation progresses, a hot patch on the base triggers the development of a hot plume of fluid rising to the surface (top right). The head of the plume reaches the surface midway between the upwelling on the left and downwelling on the right (bottom left). The tail of the plume, however, is swept into the upwelling on the left edge (bottom right).

The images were produced using the interactive graphics package Application Visualization System (AVS) at Los Alamos National Laboratory, Institute of Geophysics and Planetary Physics (IGPP). The AVS system permits rapid visual analysis of the large quantity of output from these three-dimensional, time-dependent calculations.—C. W. Gable, *Earth and Environmental Sciences, Los Alamos National Laboratory*; C. Kincaid, *Graduate School of Oceanography, University of Rhode Island*; S. Sacks, *Carnegie Institution of Washington, Department of Terrestrial Magnetism*

Table of Contents

General Information	3
Summary Chart	12
Session Highlights.....	21
Meeting Abstracts	45
Union	45
Atmospheric Sciences	60
Geodesy	79
Geomagnetism and Paleomagnetism.....	87
Hydrology.....	105
Mineralogical Society of America	141
Ocean Sciences.....	145
Planetology.....	173
Seismology.....	193
SPA-Aeronomy.....	216
SPA-Solar and Heliospheric Physics.....	234
SPA-Magnetospheric Physics.....	249
Tectonophysics	272
Volcanology, Geochemistry, and Petrology.....	323
AGU 1991 Fall Meeting Additional Abstracts.....	398
Author Index	377

The 1992 Spring Meeting abstract volume is published as a supplement to *Eos*, Transactions, American Geophysical Union, by the American Geophysical Union, 2000 Florida Avenue, N.W., Washington, DC 20009, USA. Second-class postage paid at Washington, D.C., and at additional mailing offices. POSTMASTER: Send address changes to *Eos*, American Geophysical Union, 2000 Florida Avenue, N.W., Washington, DC 20009, USA. Subscription price to regular members is included in annual dues (\$20 per year).

Copyright 1992 by the American Geophysical Union. Material in this publication may be photocopied by individual scientists for research or classroom use. Permission is also granted to use short quotes, figures, and tables for publication in scientific books and journals. For permission for any other uses, contact the AGU Publications Office.

Eos Staff: A. F. Spilhaus, Jr., Editor in Chief; Stephen Cole, Managing Editor; M. Catherine DeVito, Copy Editor

Meetings Staff: Mary Ann Emely, Director of Membership and Meetings; Brenda L. Weaver, Head of Meetings; Christine Hooke, Meetings Program Manager; Steven Bell, Meetings Secretary

Production Staff: Ronald Scott, Assistant Production Manager; Judy Castagna, Production Coordinator; Don Hendrickson, Dae Sung Kim, Elizabeth Caesar, Nancy Sims, Renee Winfield, Artists

A31C-9 1055h

An Analysis of Solar Transmission Measurements Over the South Atlantic Ocean During SABLE 89

D.R. Longtin (SPARTA, Inc., 24 Hartwell Avenue, Lexington, MA 02173)

G.G. Koenig (Geophysics Directorate, Phillips Laboratory, Hanscom AFB, MA 01731)

J.R. Hummel (SPARTA, Inc., 24 Hartwell Avenue, Lexington, MA 02173)

(Sponsor: J.R. Hummel)

SABLE, the South Atlantic Backscatter Lidar Experiment, is a joint effort between the Geophysics Directorate of the Phillips Laboratory and the Royal Signal and Radar Corps. In the summer of 1989, a series of aerosol backscattering measurements were made at and near Ascension Island (7.97°S, 14.40°W). Supporting instrumentation for SABLE 89 included a EK/EG&G solar transmissometer which was located on Ascension Island. The instrument measured solar transmission at 532 nm versus time and transmission across the solar spectrum.

This paper presents an analysis of data taken with the solar transmissometer. As an independent check, transmission data are first validated using the Langley method. Next, the solar transmissometer data are used to study the properties of cirrus and boundary layer cumulus clouds that passed in front of the sun while the instrument was working. The data clearly illustrate the presence of thin spots and edges of clouds that are generally assumed to be optically thick. Finally, transmission data are used to estimate the thicknesses of clouds as well as the wavelength dependence of maritime aerosol extinction at Ascension Island.

Research Supported by Contract F19628-91-C-0093

A31C-10 1110h

The LATAS Coherent Lidar - For Avionics and Atmospheric Measurements

P.H. Davies, J.M. Vaughan, D.W. Brown, R. Callan, R. Foord and D.J. Wilson (Defence Research Agency, RSRE, St Andrews Road, Malvern, Worcs WR14 3PS, UK)

S.B. Alejandro and G.G. Koenig (Phillips Laboratory, Air Force Systems Command, Hanscom AFB, MA 01731, USA)

The Laser True Airspeed System (LATAS) lidar developed by RSRE and RAE was originally mounted in an HS125 executive jet type aircraft and is now installed in a Canberra (B-57) aircraft. The coherent lidar itself incorporates a 3-4 Watt CW CO₂ laser at 10.6 micrometers, a 15cm germanium transmitting and receiving telescope, a cooled QMT detector and surface acoustic wave signal processing and spectral integration. The lidar head and processing units weigh approximately 25kg each. During its long period of operation the equipment has proved exceptionally reliable and rugged. The few faults that have developed have usually been associated with the electronics rather than electro-optics. Very extensive calibration studies have been carried out on the system and establish quantum limited performance. Examples of measurements in a wide range of conditions will be outlined including observations of severe thunderstorm wind shear associated with microbursts, pressure error measurements and signals observed in cloud and heavy rain. Most recently extensive measurements of atmospheric backscatter from aerosols have been conducted over the North and South Atlantic. For this collaborative programme the high ceiling of the aircraft (over 15km) and the sensitivity of the lidar (down to $5 \times 10^{-12} \text{ m}^{-1} \text{ sr}^{-1}$) have been very valuable.

A32A CC: 407 Wed 1330h Clouds and Radiation Posters Presiding: A Marshak, SSAI

A32A-1 1330h POSTER

On the Use of Artificial Intelligence for Cloud Classification

R.G. Wardell and R.A. Sheldon (Both at: LORAL AeroSys, 7375 Executive Place, Seabrook, Maryland 20706; 301-805-0462)

A critical parameterization for global radiation balance models is cloud cover. Minimally, grid based classifications are required for three classes: clear conditions; reflective and warm towards space cumulus clouds; and less reflective and cool towards space cirrus clouds. Satellite observations provide necessary spatial and temporal coverage to facilitate the classifications, but the relative scarcity of skilled nephologists limits the utilization of satellite data.

A prototype system, Satellite Image Analysis using Neural Networks (SIANN), has been developed to address the issue above. Conventional image processing techniques are used to derive input vectors for the neural networks. The human expert's knowledge is captured during the training process for the neural

network, which then can be automatically applied to similar scenes. Neural networks are appropriate for approximating complex, non-linear systems, are distribution-free, and are tolerant to errors in input data.

Limitations have been discovered during experimentation; additional artificial intelligence techniques promise to remove these. Embedding numerous neural networks within an expert system will improve the generality of the system. Genetic algorithms systematize trial-and-error searches for the optimum set of input features. Self-organizing neural networks may reduce the subjectivity of the training process. Non-technical issues include recognition of the techniques by the scientific community, but also the potential for uncritical acceptance of computer generated results.

A32A-2 1330h POSTER

Mount Pinatubo Stratospheric Aerosol Perturbation Measured by Northern Mid-Latitude Solar Photometers

Nels R. Larson and Edward W. Kleckner (Pacific Northwest Laboratory, Richland, WA 99352; 509-376-4333)

Joseph J. Michalsky and Lee C. Harrison (Atmospheric Sciences Research Center, SUNY, Albany, NY 12205; 518-442-3809)

Donald Nelson (NOAA-ERL, 325 Broadway, Boulder, CO 80303; 303-497-6662)

Atmospheric aerosol optical depths are routinely measured by solar photometers at Pacific Northwest Laboratory (PNL) in Washington State, Atmospheric Sciences Research Center (ASRC) in New York, and Environmental Research Laboratory (ERL) in Colorado. These sites have a record of optical depths extending back into times when the stratosphere was essentially unperturbed by major volcanic eruptions. Since the June 1991 eruptions of Mount Pinatubo in the Philippines, a large increase in aerosol loading has been observed above the sites. By subtracting the background aerosol optical depths from the volcanically perturbed aerosol optical depths, the amount of stratospheric aerosol loading caused by the volcano is determined for each site. Optical depths are measured at five wavelengths at PNL by a sun-scanning photometer and in one broad mid-visible band by rotating shadowband photometers at PNL, ASRC, and ERL. These data sets are examined together to elicit the spatial and temporal behavior of the Pinatubo aerosol clouds above mid-latitude North America.

Major funding of this research is provided by the U.S. Department of Energy; at PNL by the Office of Basic Energy Sciences, Geosciences Program, and at ASRC by the Office of Health and Environmental Research, Quantitative Links Program. Pacific Northwest Laboratory is operated for the U.S. Department of Energy by Battelle Memorial Institute under Contract DE-AC06-76RL0 1830.

A32A-3 1330h POSTER

Effect of Marine Stratospheric Ozone on TOMS Ozone in the Tropical Eastern Atlantic

A.M. Thompson, K.E. Pickering (NASA/Goddard Space Flight Center, Code 916, Greenbelt, MD 20771; 301-286-2629)

D.P. McNamara (Applied Research Corp., Landover, MD 20785)

The algorithm used to derive total O₃ in cloudy regions from the TOMS (Total Ozone Mapping Spectrometer) instrument is based on the measured reflectivity and a climatological cloud top height. We have been using TOMS data to study ozone off the coast of west Central Africa, which is a region of persistent marine stratocumulus. Because these clouds are lower than the mean cloud height assumed by the TOMS algorithm, this introduces an error into the assumed below-cloud ozone amount. Consequently, TOMS total ozone for these regions tends to be too high. This was confirmed by examination of TOMS, TOMS reflectivity data, and the ISCCP cloud record for the study period (September and October 1989) and the SBUV THIR (Temperature, Humidity Infrared Radiometer) data from September and October 1979. The difference in SBUV ozone with THIR and without THIR, which is a measure of the ozone discrepancy, is nearly linear with reflectivity in the region between 0° and 25°S over the Eastern Atlantic. We use this relationship to correct TOMS ozone for the 1989 study period.

Universities Space Research Association.
This research was done under contract at Goddard Space Flight Center, Greenbelt, Maryland.

A32A-4 1330h POSTER

Effects of Aerosols and Clouds on Solar Radiative Transfer & Tropospheric Chemistry

Y. Lu and M.A.K. Khalil (Global Change Research Center, Dept. of Environmental Science and Engineering, Oregon Graduate Institute, Beaverton, OR 97006; 503/690-1093)

Almost all aerosols and clouds reside in the troposphere, which comprises 80% to 85% of the total atmosphere. The levels of many trace gases and free radicals in this region are highly sensitive to solar intensity since most atmospheric chemical reactions are initiated by solar radiation. We have developed a radiative transfer model for multiple scattering plane-parallel atmospheres to calculate the actinic flux at different wavelengths, solar zenith, and altitude values, aimed at determining the effect of aerosols on solar radiative transfer at ultraviolet wavelengths. Our results show that, in ambient air, the contribution of aerosols

is usually small compared to O₃ absorption and molecular scattering. It appears to be relatively important for a few photodissociation reactions such as the photolysis of NO₂. In polluted environments, however, the effect of aerosols could be stronger than the effects of O₃ absorption and Rayleigh scattering. Clouds generally play a significant role in solar radiative transfer.

A32A-5 1330h POSTER

Sea-Surface Temperature and the Solar Irradiance in the Tropics

H.L. Dharma (University of the District of Columbia, Washington, DC 20008)

H.L. Kyle (NASA/Goddard Space Flight Center, Greenbelt, MD 20771)

In the mean, both in the tropics and at higher latitudes, an increase in the regional solar irradiance is associated with an increase in the sea-surface temperature (SST). However, closer study shows that a combination of variable cloud cover and energy transport mechanisms produce complex regional differences. This is particularly true in the tropics. The Nimbus-7 Earth Radiation Budget (ERB) and Cloud datasets are used to examine seasonal changes for 1 year (May 1979 through June 1980). The effect of changes in both the absorbed shortwave and the net radiation on the SST along the equator vary greatly from region to region. In the warm water pool in the western Pacific, there is little seasonal change in the SST. Clouds appear to act as a thermostat, thickening as the solar irradiance increases and thinning as it decreases. In the cooler eastern Pacific, there is a stronger relationship between the net radiation and the SST. The strongest tie appears along the west coast of South America where the low stratus cloud cover varies inversely with the solar irradiance.

A32A-6 1330h POSTER

Long-Term Earth Radiation Budget Observations

H.L. Kyle (NASA/Goddard Space Flight Center, Greenbelt, MD 20771)

P.E. Arduini (Research and Data Systems Corporation, Greenbelt, MD 20770)

J.R. Hickey (The Eppley Laboratory, Inc., Newport, RI 02840)

A nearly continuous broad spectral band record of the Earth's albedo and outgoing longwave radiation (OLR) exists from July 1975 to the present and the measurement program is continuing. The measurements were made by the Nimbus-6 and -7 satellites and also by the Earth Radiation Budget Experiment (ERBE) wide field of view (WFOV) sensors. Several investigators have used these data to examine important climate problems such as the effects of cloud and surface conditions on the Earth's radiation budget (ERB), determination of the net solar irradiance at the ocean surface, annual and interannual variations in both the shortwave and OLR (this includes both El Niño/Southern Oscillation and volcanic stratospheric aerosol perturbations), equator-to-pole and cross-midlatitude energy transport, and the relationship between variations in the surface temperature, the Earth's radiation budget, and the total solar irradiance. The present datasets are not optimal because different procedures were used in processing the Nimbus-6, -7, and ERBE products and it is not presently planned to process and release all the Nimbus-7 measurements. To date, only WFOV sensors have proved their ability to make accurate, long-term ERB measurements. However, some effort is still needed to join the different datasets.

A32A-7 1330h POSTER

Calculation of UV-B Exposure at the Earth's Surface

D.H. Charache, V.J. Abreu, W.R. Skinner, and W.R. Kuhn
(All at: Dept. of Atmospheric, Oceanic and Space Science, University of Michigan, Space Research Building, 2455 Hayward, Ann Arbor, MI 48109)
A. Bucholtz (Atmospheric Physics Research Branch, NASA-Ames Research Center, Moffett Field, CA 94035)

Existing cloud, aerosol, and ozone databases were incorporated into a multiple scattering radiative transfer model to determine the UV-B flux reaching the surface of the Earth. Climatological data on sky coverage and frequency of occurrence of various cloud types were used to incorporate up to three cloud layers into the model. Boundary layer aerosol and TOMS ozone databases were also employed into the model calculations. The UV-B spectrum obtained was then weighted with an erythral action spectrum to estimate the effective biological exposure for erythema. Results show an increase in UV-B exposure between pre- and post-ozone depletion years; calculations suggest that a decrease in total column density of ozone of 1% leads to an increase in erythral exposure by approximately 2%. In this presentation we will review the model, the databases, and the sensitivity of UV-B flux at the surface to anthropogenic aerosol loading, increased tropospheric ozone concentrations, and varying meteorological cloud conditions.